

**SILICATE AND SULPHIDE MINERAL ASSEMBLAGES
AND METAMORPHIC FABRICS FROM PELITES IN THE
CONTACT AUREOLE OF THE SOUTH MOUNTAIN BATHOLITH,
HALIFAX AREA, NOVA SCOTIA**

Bonnie L. Betts-Robertson

Submitted in Partial Fulfillment of the Requirements
for the Degree of Bachelor of Science, Honours
Department of Earth Sciences
Dalhousie University, Halifax, Nova Scotia
March, 1998

Distribution License

DalSpace requires agreement to this non-exclusive distribution license before your item can appear on DalSpace.

NON-EXCLUSIVE DISTRIBUTION LICENSE

You (the author(s) or copyright owner) grant to Dalhousie University the non-exclusive right to reproduce and distribute your submission worldwide in any medium.

You agree that Dalhousie University may, without changing the content, reformat the submission for the purpose of preservation.

You also agree that Dalhousie University may keep more than one copy of this submission for purposes of security, back-up and preservation.

You agree that the submission is your original work, and that you have the right to grant the rights contained in this license. You also agree that your submission does not, to the best of your knowledge, infringe upon anyone's copyright.

If the submission contains material for which you do not hold copyright, you agree that you have obtained the unrestricted permission of the copyright owner to grant Dalhousie University the rights required by this license, and that such third-party owned material is clearly identified and acknowledged within the text or content of the submission.

If the submission is based upon work that has been sponsored or supported by an agency or organization other than Dalhousie University, you assert that you have fulfilled any right of review or other obligations required by such contract or agreement.

Dalhousie University will clearly identify your name(s) as the author(s) or owner(s) of the submission, and will not make any alteration to the content of the files that you have submitted.

If you have questions regarding this license please contact the repository manager at dalspace@dal.ca.

Grant the distribution license by signing and dating below.

Name of signatory

Date



Dalhousie University

Department of Earth Sciences

Halifax, Nova Scotia

Canada B3H 3J5

(902) 494-2358

FAX (902) 494-6889

DATE March 16th, 1998

AUTHOR Bonnie L. Betts-Robertson

TITLE SILICATE AND SULPHIDE MINERAL ASSEMBLAGES AND METAMORPHIC

FABRICS FROM PELITES IN THE CONTACT AUREOLE OF THE SOUTH

MOUNTAIN BATHOLITH, HALIFAX AREA, NOVA SCOTIA

Degree B.Sc. Convocation May Year 1998

Permission is herewith granted to Dalhousie University to circulate and to have copied for non-commercial purposes, at its discretion, the above title upon the request of individuals or institutions.

Bonnie L. Betts-Robertson
Signature of Author

THE AUTHOR RESERVES OTHER PUBLICATION RIGHTS, AND NEITHER THE THESIS NOR EXTENSIVE EXTRACTS FROM IT MAY BE PRINTED OR OTHERWISE REPRODUCED WITHOUT THE AUTHOR'S WRITTEN PERMISSION.

THE AUTHOR ATTESTS THAT PERMISSION HAS BEEN OBTAINED FOR THE USE OF ANY COPYRIGHTED MATERIAL APPEARING IN THIS THESIS (OTHER THAN BRIEF EXCERPTS REQUIRING ONLY PROPER ACKNOWLEDGEMENT IN SCHOLARLY WRITING) AND THAT ALL SUCH USE IS CLEARLY ACKNOWLEDGED.

ABSTRACT

Contact metamorphism resulting from intrusion of the South Mountain Batholith (SMB) at 372 Ma produced textural and mineralogical changes in rocks of the Meguma Supergroup. A detailed petrographic study of the contact aureole of the Halifax Group was conducted to determine the relationship between sulphide and silicate mineral assemblages, and the relationship of these assemblages to metamorphic fabrics.

Field relations indicate that rocks in the contact aureole of the SMB contain structures formed during regional deformation which were overprinted by contact metamorphism. The samples collected were grouped according to silicate porphyroblast assemblage into six groups which show systematic variation with distance from the contact. Sulphide mineral assemblages show little to no variation with distance from the contact. Microprobe analyses of both sulphides and silicates show little compositional variation throughout the study area. Petrographic analyses show that regional cleavage (S1) developed before cordierite growth and was reactivated to form a syn-emplacement fabric (S2) prior to andalusite growth. Maximum P-T conditions are estimated at 2.5-3.0 kbar and 590-620°C, using Pattison and Tracy's (1991) phase diagram for pelites.

The silicate mineral assemblage of Halifax Group rocks in the contact aureole of the SMB varies systematically with distance from the contact and is therefore thermally controlled. The sulphide mineral assemblage, as determined from petrography, mineral chemistry, and field data is lithologically controlled in the contact aureole and therefore has no direct relationship to contact metamorphism. In conclusion, the complicated relationships of porphyroblasts and fabrics in the contact aureole of the SMB result from deformation and thermal effects superimposed on lithological variations.

KEYWORDS: South Mountain Batholith, Meguma Supergroup, contact metamorphism, pelites, silicates, sulphides.

Table of Contents

	page
Abstract	i
Table of Contents	ii
List of Figures	iv
List of Tables	v
Acknowledgements	vi
Chapter 1: Introduction	1
1.1 Introduction	1
1.2 Objectives	2
1.3 General Geology	4
1.4 Previous Work	8
1.5 Organization	9
Chapter 2: Field Relations	10
2.1 Introduction	10
2.2 Lithologies	10
2.3 Structure	13
2.4 Summary	16
Chapter 3: Petrography	17
3.1 Introduction	17
3.2 Group Descriptions	17
3.3 Mineral Chemistry	25
3.3.1 Sulphide Mineral Assemblage and Grain Size	28
3.3.2 Silicate Mineral Assemblage	28
3.4 Generalized Silicate and Sulphide Relationships	31

Chapter 4: Interpretation and Discussion	36
4.1 Introduction	36
4.2 Porphyroblast Growth and Fabric Development	36
4.3 Changes in Mineralogy with Distance from the Contact	41
4.4 Pressure-Temperature Conditions	45
Chapter 5: Conclusions	47
5.1 Conclusions	47
5.2 Future Work	48
References	49
Appendix A: Petrographic Descriptions	A1
Appendix B: Electron Microprobe Method	B1
Appendix C: Microprobe Data	C1

List of Figures

	page
1.1 Regional Map	3
1.2 Location Map	5
1.3 Stratigraphic column	7
2.1 Map of study area including sample sites	11
2.2 Corrugated surface	15
2.3 Fault	15
2.4 Concretions	15
3.1 Andalusite and fibrolite	19
3.2 Fibrolite	19
3.3 Andalusite	21
3.4 Andalusite and biotite	21
3.5 Andalusite and cordierite	23
3.6 Coarse quartz-rich lithology	23
3.7 Parallel alignment of sulphides	24
3.8 Parallel alignment of elongate grains	24
3.9 Colliform texture	26
3.10 Cordierite and sulphides and texture	26
3.11 Andalusite and cordierite	27
3.12 Percent iron versus distance	27
3.13 Samples by group versus distance	29
3.14 Modal percent total sulphides versus distance	29
3.15 Modal percent sulphide by type versus distance	30
3.16 Sulphide grain size versus distance	30
3.17 Modal percent silicates versus distance	32
3.18 AFM diagram	34
4.1 Biotite parallel cleavage	37
4.2 Cordierite inclusions parallel cleavage	37
4.3 Biotite and sulphides deflected around cordierite	39
4.4 Andalusite cutting cordierite	39
4.5 Andalusite parallel and perpendicular to cleavage	40
4.6 Cordierite-Andalusite-Deflection	40
4.7 Random mica in retrograde cordierite	42
4.8 Temporal sequence of metamorphism	41
4.9 Phase Diagram	46

List of Tables

3.1	Summary data table	18
3.2	Silicate mineral assemblage fields	31
3.3	Sample data by distance from the contact	35

ACKNOWLEDGEMENTS

I would like to thank my supervisor, Dr. Becky Jamieson, for her guidance and support over the past year. I would also like to thank Dr. Martin Gibling for advice, encouragement, and patience. I also thank Nick Wilson for help with sulphide petrography, and AUTOCAD©.

I would like to thank Gordon Brown for thin section preparation, and Bob MacKay for microprobe assistance.

Thank you to Pradeep Bhatnagar for enjoyable days in the field and for someone to compare notes with.

I would like to thank my classmates for their constant support, encouragement, understanding, and laughter, it would not have been possible without them!

Finally, thanks to my family for teaching me that I could do anything if I put my mind to it.

CHAPTER 1

Introduction

1.1 Introduction

Contact metamorphism is recognized by changes in texture and mineralogy of country rock resulting from the intrusion of an igneous body. Intrusion of the South Mountain Batholith produced textural and mineralogical changes in rocks of the Meguma Supergroup. This study is focused on textures and mineralogy of the contact aureole of the South Mountain Batholith.

The Devonian South Mountain Batholith of southern Nova Scotia is the largest granitoid intrusive complex in the Appalachians (Abbott, 1989). The South Mountain Batholith intruded the Meguma Supergroup, a thick Cambrian-Ordovician siliciclastic sequence deposited on the continental margin of Gondwana (Schenk, 1995b). The Halifax Group, the younger unit of the Meguma Supergroup, is Early Ordovician in age and includes black shale interbedded with minor greywacke (Schenk, 1991). The Goldenville Group is late Cambrian to Early Ordovician in age and includes quartzose to feldspathic metawacke interbedded with green to gray shale (Schenk, 1991). The Halifax Group has a minimum thickness of ~7km and includes five conformable formations (Schenk, 1995a). Beginning with the oldest, these formations are: Mosher's Island, Cunard, Feltzen, Delanceys, and Rockville Notch. Intrusion of the South Mountain Batholith produced contact metamorphism, defined as the changes caused by heating in proximity to an intrusive body

(Yardley, 1989). Contact metamorphism of the Halifax Group as a result of intrusion of the South Mountain Batholith is the focus of this study (fig. 1.1).

The Meguma Supergroup, previously known as the Meguma Group, was recently elevated to Supergroup status, and the Goldenville and Halifax Formations are now considered Groups (Schenk, 1995b). The new nomenclature is used throughout the thesis.

1.2 Objectives

The objective of this thesis is to complete a detailed petrographic study of the contact metamorphic aureole of the Halifax Group, to obtain a better understanding of the relationship between the silicate and sulphide mineral assemblages, and the relationship of these assemblages to metamorphic fabrics. Figure 1.2 is a location map showing the study area which extends from Exit 2A on Highway 102 near Halifax, south to St. Margaret's Bay Road, and east to Fairmont subdivision. The area included in this study has excellent fresh exposure resulting from recent commercial development in the Bayers Lake Industrial Park, and is interesting from a structural point of view (Bhatnagar, 1998).

The thesis is an attempt to determine if a systematic change occurs in sulphide mineralogy with distance from the contact, and if so how that change correlates with changes in silicate mineralogy. In addition, the relationship between porphyroblast growth and fabrics was investigated to see if there is evidence for syn or post-metamorphic deformation. Finally, pressure-temperature conditions in the country rock

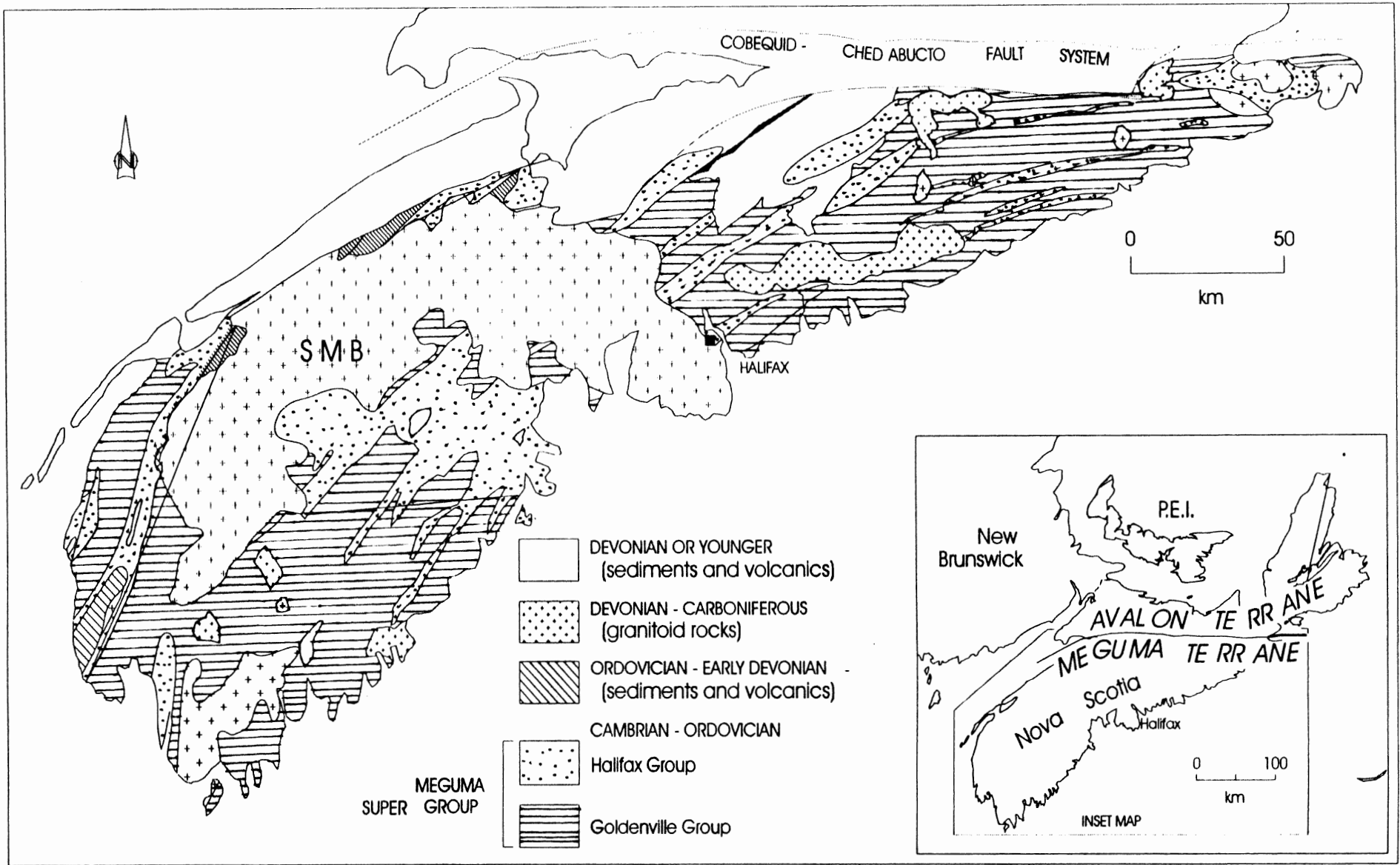


Fig. 1.1 Regional map of southern Nova Scotia showing the Meguma Supergroup and the South Mountain Batholith (SMB)..

adjacent to the intruding granite were estimated to determine emplacement conditions of the batholith, in particular depth.

1.3 General Geology

The Meguma Zone includes shales and greywackes of the Meguma Supergroup, siliciclastic and volcanoclastic strata of the Annapolis Supergroup (fig. 1.3) (Schenk, 1995a), and granitic plutons including the South Mountain Batholith (Clarke *et al.*, 1997). The Meguma Zone was the last to be accreted to the northern Appalachians (Schenk, 1983), and is separated from the Avalon Zone by the Cobequid-Chedabucto Fault (Keppie, 1982).

According to Schenk (1983), the Goldenville Group is a mid-submarine fan channel deposit, and the Halifax Group is a thick turbidite sequence, deposited on the continental slope of Gondwana. The Goldenville Group includes massive sandstones with minor interbedded shale. The Goldenville Group has a gradational contact with the Halifax Group, which includes black shales with minor interbedded greywacke.

The Meguma Supergroup was regionally deformed and metamorphosed to greenschist facies during the Middle Devonian Acadian Orogeny (Abbott, 1989). Precise $^{40}\text{Ar}/^{39}\text{Ar}$ ages of 395-388 Ma have been determined for regional metamorphism in the Mahone Bay area (Hicks, *et al.*, submitted). This deformation resulted in northeast-southwest trending regional folds (Horne *et al.*, 1992), which are truncated by the SMB, which was intruded at ca. 372 Ma (Clarke *et al.*, 1997).

The South Mountain Batholith is a composite peraluminous granitoid body that crops out over approximately 7300km² and includes 13 individual plutons which are

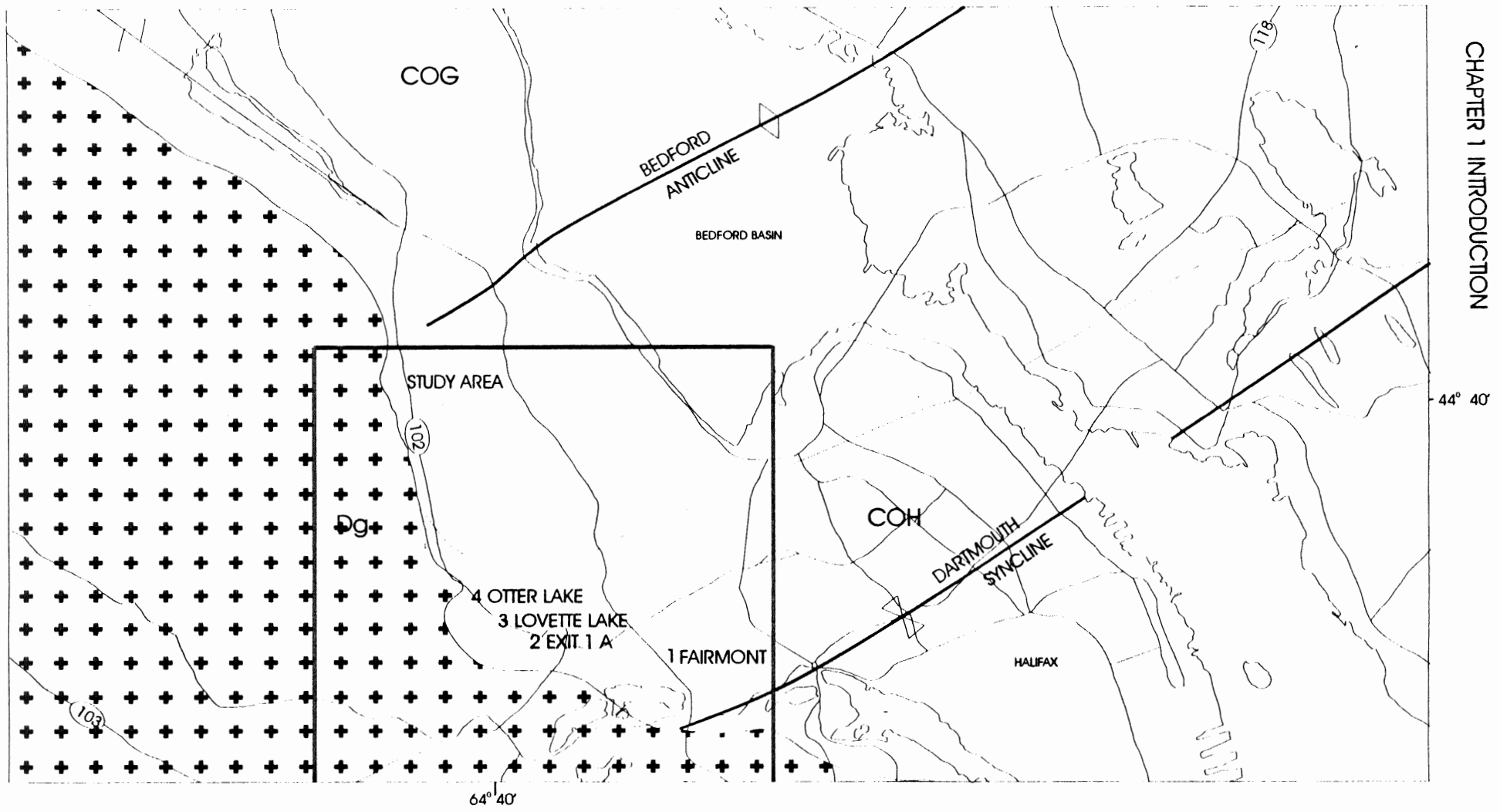
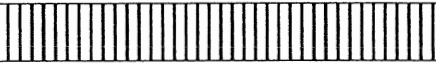
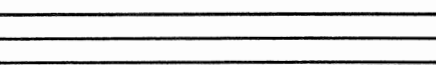
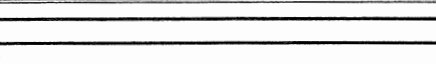
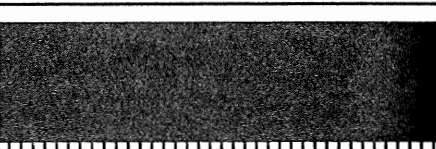

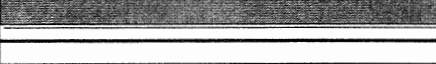

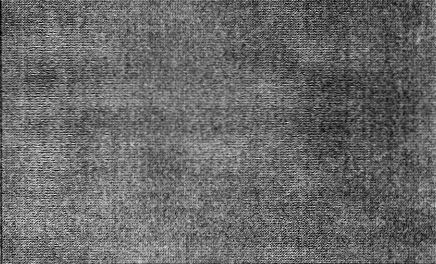


Fig. 1.2 Location map showing SMB contact and study area in Halifax. COH - Halifax Group, COG - Goldenville Group, DG - SMB. Map scale is 1 : 66,000. Modified from Gray, 1996.

grouped into two stages (1 granodiorite and monzogranite; 2 leucomonzogranite and leucogranite ;MacDonald *et al.*, 1992). Emplacement of the SMB at ca. 372 Ma (Clarke *et al.*, 1997) produced contact metamorphism of the Meguma Supergroup. Contact metamorphism of the Halifax Group at the eastern edge of the Halifax pluton of the South Mountain Batholith is the focus of this thesis.

The Meguma Supergroup may have experienced continued deformation into the Permian associated with northwest directed transpression (Horne *et al.*, 1992). This is indicated by dextral, strike-slip movement along regional fault systems (Keppie, 1982); northwest shortening of Upper Paleozoic sedimentary basins in the region (Nance, 1987); and northeast dextral shearing in the Meguma Terrane into the Permian (Dallmeyer and Keppie, 1987). Continued deformation further complicated structural features in the contact aureole of the SMB, making it difficult to distinguish regional effects from effects of emplacement. There are three possible fabrics in the contact aureole of the SMB including S1, a pre-emplacement fabric such as regional cleavage (observed); S2, a syn-emplacement fabric which is directly related to granite intrusion and is very localized (observed); and S3, a post-emplacement fabric that may be related to late stage flexural slip folding or dextral transpression.

Regional structures played an important role in the emplacement and evolution of the South Mountain Batholith (MacDonald *et al.*, 1992). Northeast-trending regional faults were active during plutonism and may have controlled emplacement of some plutons which comprise the SMB (Horne *et al.*, 1992). Some stage 1 plutons show weakly developed primary flow features parallel to regional structures, suggesting that regional Acadian stress was active during initial plutonism (MacDonald *et al.*, 1992). The northeast-trending,

Time	Units	Thickness	Lithology	Environment
Ordovician	Rockville Notch	32		Slope
	Delanceys	1850		
	Feltzen	2000		
	Cunard	8000		
	Mosher's Is.	500		
Cambrian	West Dublin	1000		Fan
	Risser's Beach	1000		
	New Harbour	+7000		

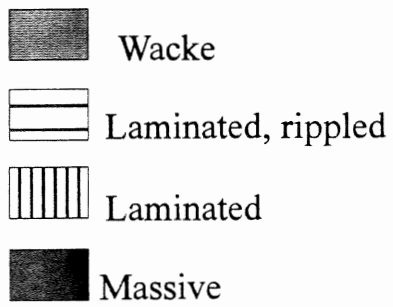


Fig. 1.3 Stratigraphic column of Goldenville and Halifax Groups of the Meguma Supergroup. Thicknesses measured in meters, environment of deposition interpretation by Schenk, Figure is modified from Schenk, 1995.

elongate shape of some plutons may be the result of structural control by emplacement along pre-existing structures in the country rocks (Horne *et al.*, 1992).

The nature of emplacement of the SMB is still poorly understood. Three models of emplacement and origin of the SMB are in the literature, including McKenzie and Clarke (1975), Charest *et al.* (1985), Clarke and Muecke (1985), who argue emplacement as a single comagmatic body; Smith and Turek (1976), Smith (1979), emplacement as a series of plutons coalescing to form the SMB; Richardson *et al.* (1989), plutonism in stages; and Benn *et al.* (1997), emplacement as a syn-tectonic laccolithic complex.

1.4 Previous work

Although both the South Mountain Batholith and the Meguma Supergroup rocks are well studied, their contact is less well understood. MacDonald *et al.* (1992) noted andalusite and cordierite in the country rocks surrounding the South Mountain Batholith, but did not study the contact aureole in detail.

Jamieson (1974) studied the contact aureole near Mount Uniacke to define thermal metamorphic stages and assimilation of xenoliths and to define effects of chemical exchange. This study resulted in the definition of six progressive stages of xenolith assimilation and determined that chemical exchange effects are observed in both the xenoliths and the granite.

Mahoney (1996) conducted a detailed petrographic study of the contact aureole at ten localities around the South Mountain Batholith. This study concluded that the contact metamorphic aureole of the SMB is well developed around the margin against both stage 1

and stage 2 plutons except along the northern side. The aureole is best developed in Halifax Group rocks and ranges in width from 0.4 to 3 km. Thermobarometry indicated country rock temperatures of 500^o to 550^oC +/- 40^oC and pressures between 3.0 and 3.8 kbar.

Robinson (1996) looked at acid rock drainage in the contact aureole, including the area sampled for this study, and concluded that the dominant sulphide mineral in Halifax Group rocks is monoclinic pyrrhotite which shows little to no regional variation in composition. She further concluded that rocks at the sites studied are net acid producers, and suggested that Halifax Group rocks are potential acid rock drainage producers regionally.

Gray (1996) looked at the structure of the contact aureole in the Goldenville Group around Kearney Lake and concluded that local structures are the result of granite emplacement and that contact metamorphism and deformation are closely linked locally. A detailed petrographic study of the contact aureole of the South Mountain Batholith in the Halifax Group has not previously been conducted within the area included in this study.

1.5 Organization

Chapter 2 of this thesis deals with observed field relations, lithologies, and structure within the Halifax Group. Chapter 3 discusses the petrography of samples based on analysis of normal and polished thin sections, as well as microprobe data. Chapter 4 includes interpretation and discussion of results presented in this study followed by conclusions in Chapter 5.

CHAPTER 2

Field Relations

2.1 Introduction

This chapter describes lithological and structural features of the Halifax Group at the eastern edge of the South Mountain Batholith (SMB) as determined by previous workers and the author. The contact metamorphic aureole of the South Mountain Batholith contains structural, textural, and mineralogical features associated with intrusion of the batholith and earlier regional metamorphism. Structural features include pre-SMB northeast-trending regional folds and an east-trending anticline near the SMB contact. Cleavage is well developed in Halifax Group rocks, however it is not well preserved in the contact aureole. Mineralogical features include abundant andalusite, cordierite, and sulphides near the contact and these phases show increasing grain size toward the contact. The textural relationship between growth of metamorphic minerals, including sulphides, and pre-syn and post-metamorphic fabrics is of particular importance in this study since it provides information on time of fabric formation relative to contact metamorphism.

2.2 Lithologies

Field data were collected by examining outcrops exposed near the SMB contact in the study area (fig. 2.1). Outcrops showed a range in degree of weathering from relatively

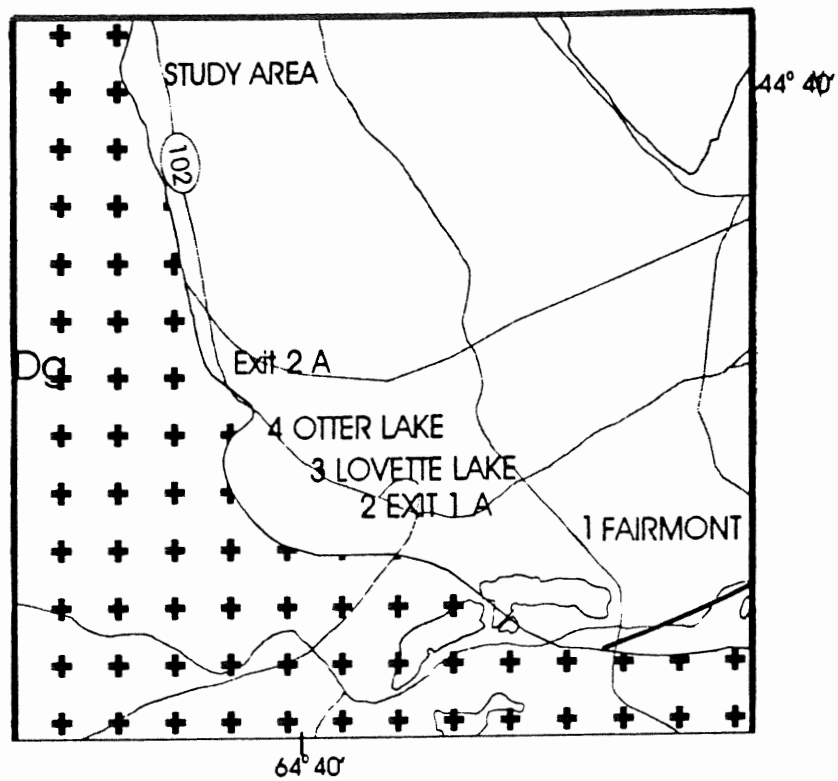


Fig. 2.1 Map of study area including sampling localities; 1. Fairmont subdivision, 2. Exit 1A off Highway 102, 3. Lovette Lake Court (Metro Self Storage), 4. Otter Lake Crescent. Map scale is 1: 52,000. Modified from Gray, 1996.

Both oriented and non-oriented samples were collected from the study area. Twenty-three samples were taken at distances from about 100m up to approximately 1300 m from the contact, and at textural and mineralogical points of interest, such as locations with abundant coarse-grained andalusite or cordierite and locations rich in sulphide.

This study area includes rocks of the Mosher's Island Formation and the Cunard Formation of the Halifax Group of the Meguma Supergroup (Schenk, 1995b). Sample BB-97-1 includes spessartine garnet at the contact with the SMB, where it intruded Mn-rich rocks of the Goldenville-Halifax Transition zone (GHT) (Schenk, 1995a), which are equivalent to the Mosher's Island Formation. This lithology is located in the study area near Exit 2A on Highway 102.

Lithologies of the Cunard Formation sampled include fine, parallel laminated dark gray slates; massive, gray pelites; fissile, sulphide-rich pelite; and hornfels. Abundant andalusite, cordierite, and sulphides form coarse-grained, idioblastic crystals within a fine-grained matrix.

A fissile, sulphide-rich layer ~20 cm thick is associated with a massive aluminous layer throughout the study area. Andalusite and cordierite are both abundant throughout the study area. Grain size increases toward the contact, with andalusite crystals up to 1cm long at the contact. Preferred orientation of andalusite is parallel to bedding (east-west) near the contact (within 550 m) where regional cleavage is annealed, and parallel to regional cleavage (northeast-southwest) where this is preserved further away from the contact.

2.3 Structure

Minor features in the Goldenville-Halifax Transition Zone include boudinaged beds, with the long axis of the boudins parallel to the dip direction of bedding planes, sulphide-rich layers, and pink garnet-rich layers. Several ~1 m wide, discordant pegmatite dykes were observed within Halifax Group slates. Bedding surfaces throughout the study area have a corrugated surface texture (fig. 2.2) sub-parallel to the bedding plane. This phenomenon is caused in some locations by discordant intrusion of granite dykelets into the country rock. These dykelets are less susceptible to erosion and stand out as ridges on the bedding plane. In other locations corrugating is the result of relict bedding being offset along annealed cleavage planes.

A brief description of outcrop-scale structures is given for each of the four major sampling localities. These localities are: 1. Fairmont subdivision; 2. Exit 1A off Highway 102; 3. Lovette Lake Court (Metro Self Storage); 4. Otter Lake Crescent. Sample locality 1 is 600-500 m from the contact, locality 2 is 500-400 m from the contact, and localities 3 and 4 are 400-100 m from the contact.

1 Fairmont subdivision outcrops are relatively fresh, with bedding following regional trends, striking east-west and dipping between 30-40° south. A small outcrop scale fold axis was measured at 078°/12°, which is also consistent with regional trends. Cleavage in the Fairmont subdivision rocks is axial planar to the regional folding at 080°/80°. The corrugated surface of bedding planes previously described is observed (fig. 2.2).

Andalusite and cordierite are both observed in outcrop, with andalusite showing preferred

orientation parallel to cleavage. Sulphides are present throughout the locality and a sulphide-rich fissile layer occurs with an aluminous layer.

2 Exit 1A off Highway 102 has excellent exposure of moderately weathered Halifax Group rocks. Some surfaces have a sulphide stained rind up to 0.5 cm thick. Bedding at this locality maintains the regional strike of 080° , but dips very steeply ($76-88^{\circ}$) to the south. Small scale boudinaged beds (3 cm thick) indicate long axes stretching parallel to the dip direction. The corrugated surface described previously is observed at this locality (fig. 2.2). Cleavage is annealed and coarse-grained andalusite is oriented parallel to bedding. Cordierite is abundant, and sulphide-rich, fissile layers also occur.

3 Lovette Lake Court (Metro Self Storage) has excellent, relatively fresh exposures of Halifax Group rocks. Bedding at this locality shows the regional east-west trend, however the beds dip steeply north. Cleavage is annealed, and the previously mentioned corrugated surface is observed (fig. 2.2). A series of discordant granite dykes ~1 m wide is present in the outcrop. A small-scale normal fault is observed (fig. 2.3), as well as small (1 cm) circular convex concretions on the bedding surface (fig. 2.4). Course-grained andalusite is abundant in outcrop.

4 Otter Lake Crescent has extensive but highly weathered outcrop of Halifax Group rocks. Bedding here is measured at $078^{\circ}/82^{\circ}$, and cleavage is annealed. Coarse andalusite is abundant in outcrop.

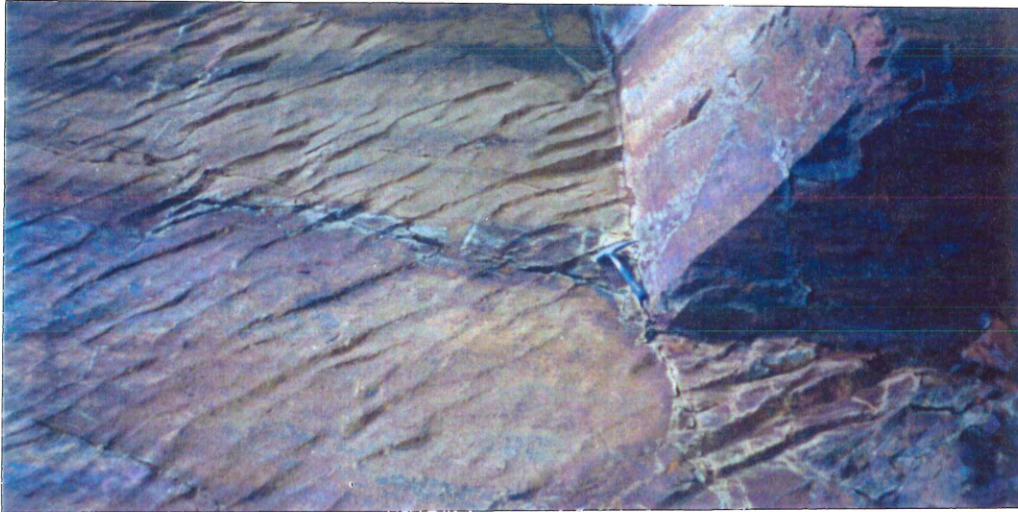


Fig. 2.2 Corrugated surface texture noted from bedding surfaces throughout the study area. Photo taken at sampling locality 3 (Lovette Lake Court). Note hammer for scale.



Fig. 2.3 Small scale (note hammer) normal fault. Photo taken at sampling locality 3.



Fig. 2.4 Circular convex concretions on bedding surface. These were observed in one outcrop only, in a more psammitic lithology.

2.4 Summary

Rocks in the contact metamorphic aureole of the South Mountain Batholith contain structures formed during regional deformation which were overprinted by contact metamorphism. For example, slaty cleavage which is well developed regionally is annealed in the contact aureole. Regional axial planar cleavage is prominent in Halifax Group rocks outside the contact aureole of the SMB, and becomes annealed within 500-400 m of the contact with the SMB.

Effects of early cleavage can still be detected within the aureole, and are also overprinted by syn-emplacement textures. Structural features in the study area are being studied in relation to the contact aureole on a larger scale to determine mode of emplacement of the South Mountain Batholith (Bhatnagar, 1998).

CHAPTER 3

Petrography

3.1 Introduction

This chapter deals with the petrography of samples as determined from microscope analysis in transmitted and reflected light. Samples taken from the study area have been categorized according to their major silicate mineral assemblages into six groups. These groups are described here in terms of characteristics common to the samples in the group. Table 3.1 gives a summary of groups which includes sample number, locations, lithology, and characteristic mineralogy. A detailed petrographic description of each sample can be found in Appendix A. Variations in mineral chemistry are also given in this chapter. Microprobe analyses can be found in Appendix C.

3.2 Group Descriptions

Group 1 samples occur 0-200 m from the contact of the SMB. These samples are fine-grained pelites with hornfels texture, and contain up to 10% fine-grained pyrrhotite. Group 1 includes samples with porphyroblasts of andalusite, and fibrolitic sillimanite, and is represented by samples BB-97-18, BB-97-15, BB-97-16, and BB-97-20. Sample BB-97-18 contains 10% chiastolite porphyroblasts up to 2 mm long, with fibrolite rimming and replacing the grains (fig. 3.1). Sample BB-97-15 contains 20% andalusite porphyroblasts up to 1 mm long also partly replaced by fibrolite (fig. 3.2). Sample BB-97-16 does not

Table 3.1 Summary of groups including sample numbers, sample locations, lithology, and gross mineralogy. For a detailed mineralogical description see Appendix A.

GROUP #	SAMPLE #	SAMPLE SITE	LITHOLOGY	SIGNIFICANT MINERALS
1	BB-97-15	Lovette Lk Court	pelite (hornfels)	andalusite, cordierite, fibrolite
	BB-97-16	Lovette Lk Court	pelite (hornfels)	andalusite, cordierite
	BB-97-18	Otter Lk Crescent	pelite (hornfels)	andalusite, cordierite, fibrolite
	BB-97-20	Otter Lk Crescent	pelite (hornfels)	andalusite, fibrolite
2	BB-97-8	Exit 1A, Hwy 102	pelite (hornfels)	andalusite, cordierite, pyrrhotite
	BB-97-10	Exit 1A, Hwy 102	pelite (hornfels)	andalusite, pyrite
	BB-97-12	Exit 1A, Hwy 102	pelite (hornfels)	andalusite, cordierite
3	BB-97-2	Fairmont	pelite	and., cord., pyrrhotite (monoclinic)
	BB-97-4	Fairmont	pelite	andalusite, cordierite
4	BB-97-11	Exit 1A, Hwy 102	pelite	pyrite
	BB-97-21	Bayers Lake Ind. Park (Kmart)	pelite	quartz, muscovite
	BB-97-22	Bayers Lake Ind. Park (Kmart)	pelite	quartz, chlorite
5	BB-97-3	Fairmont	pelite	pyrrhotite(monoclinic & hexagonal)
	BB-97-7	Dunbrack Street	pelite	cordierite, pyrrhotite (monoclinic)
	BB-97-13	Exit 1A, Hwy 102	pelite	cordierite, pyrrhotite
6	BB-97-6	Main Street	pelite	andalusite, cordierite

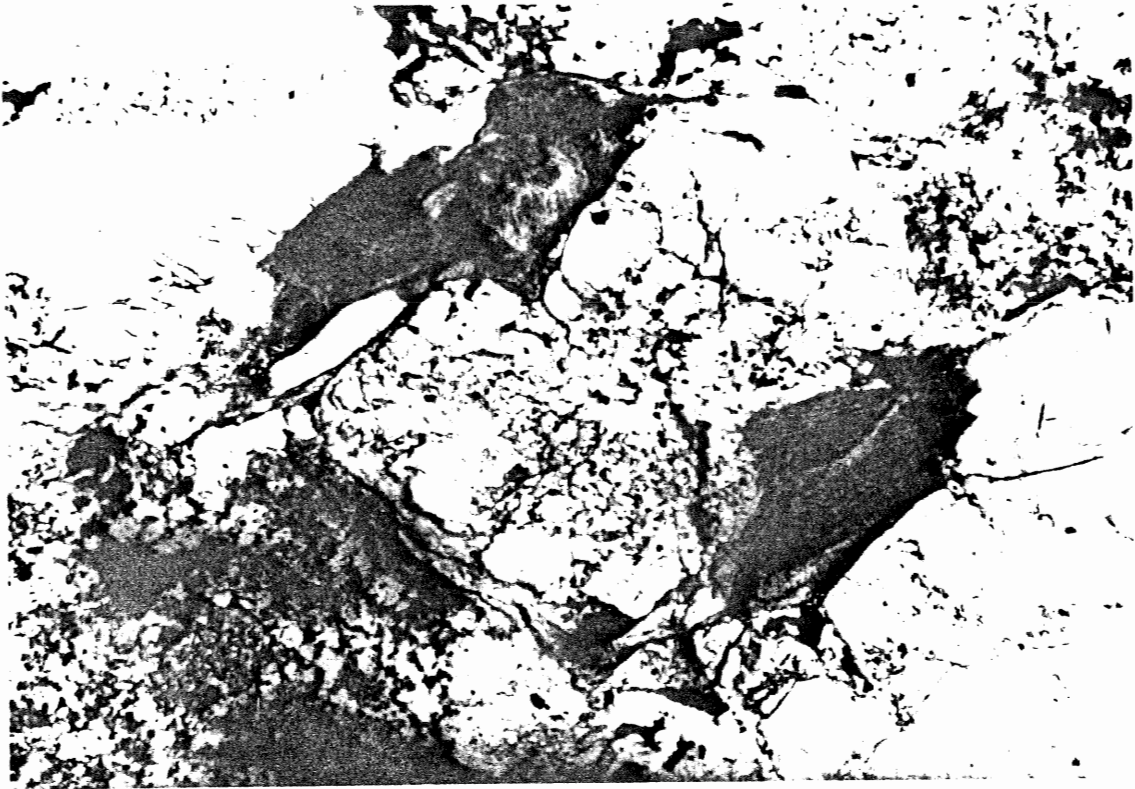


Fig. 3.1 Fibrolite rimming and replacing andalusite in sample BB-97-18. Field of view is 1 x 2 mm.

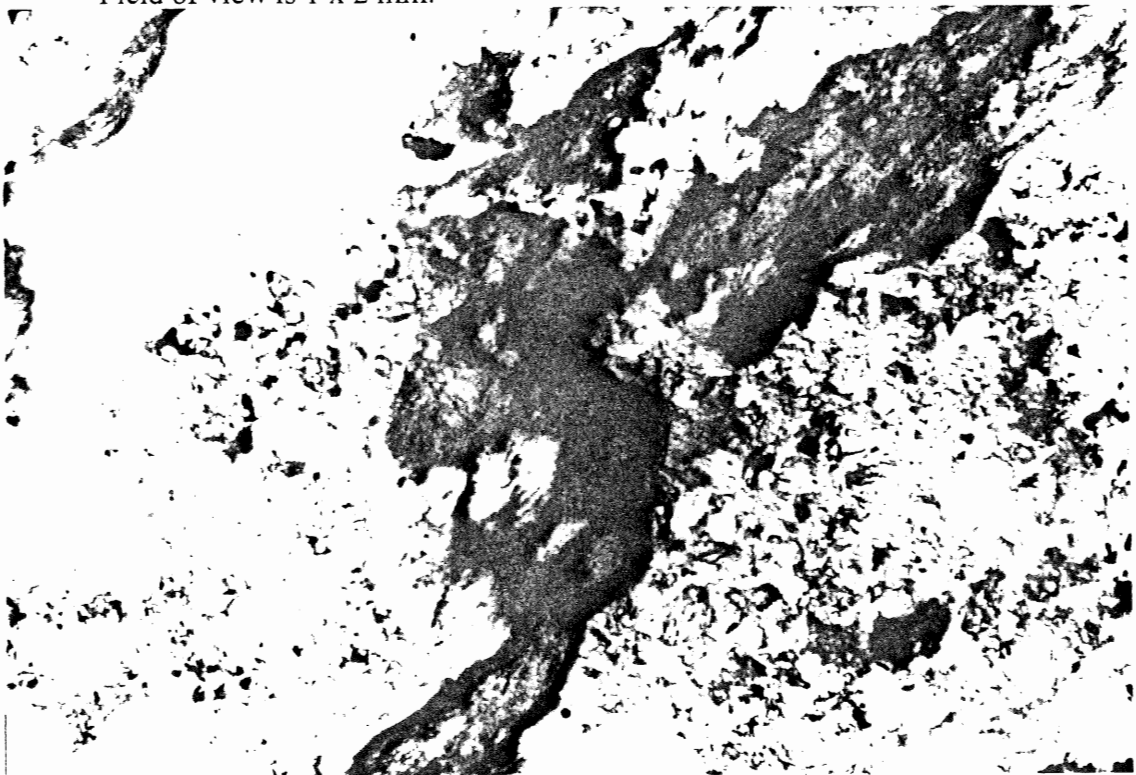


Fig. 3.2 Fibrolite in sample BB-97-15. Field of view is 1 x 2 mm.

contain fibrolite but includes other characteristics common to group 1 samples, such as porphyroblasts of andalusite (fig. 3.3).

Group 2 samples occur 380-450 m from the contact of the SMB. These are hornfelses in which parallel alignment of elongate andalusite grains defines a foliation. Group 2 includes samples with porphyroblasts of andalusite, cordierite, biotite, and sulphides, and is represented by samples BB-97-8, BB-97-10, and BB-97-12. Sample BB-97-8 contains 20% andalusite porphyroblasts 2 mm long, 10% subidioblastic cordierite porphyroblasts 1 mm in diameter, and 10% pyrrhotite. Sample BB-97-10 contains 30% chiastolite porphyroblasts up to 1 cm long (fig. 3.4), 10% cordierite, and 10% medium grained xenoblastic pyrite with minor intergrown ilmenite. Group 2 samples contain on average 25% andalusite, 17% cordierite, and 11% sulphides. Both pyrite and pyrrhotite are medium-grained (1 mm).

Group 3 samples occur 550-620 m from the contact of the SMB. Slaty cleavage (S1) is poorly developed in group 3 samples. Group 3 includes samples with porphyroblasts of andalusite, cordierite, biotite, and pyrrhotite and is represented by samples BB-97-2 (fig. 3.5) and BB-97-4. Up to 20-30% andalusite and cordierite are present in these samples which also include up to 5% monoclinic pyrrhotite. Sample BB-97-4 includes idioblastic, hexagonal cordierite crystals that are not observed in other samples. Group 3 samples have a fine-grained matrix comprising quartz, biotite, muscovite, pyrrhotite, pyrite, ilmenite, and rare chalcopyrite.

Group 4 samples occur 340-400 m from the contact of the SMB. These samples are more quartz-rich with medium-grained equant quartz in the groundmass with

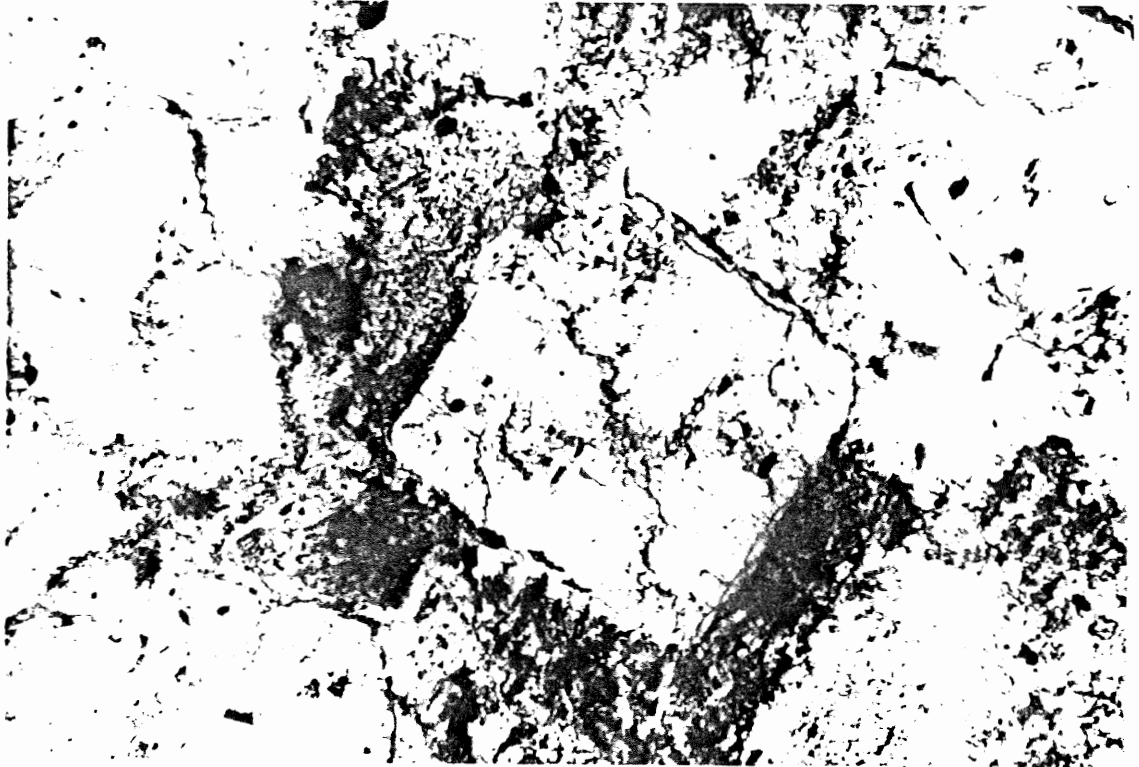


Fig. 3.3 Porphyroblasts of andalusite in sample BB-97-16. Field of view is 1 x 2 mm.

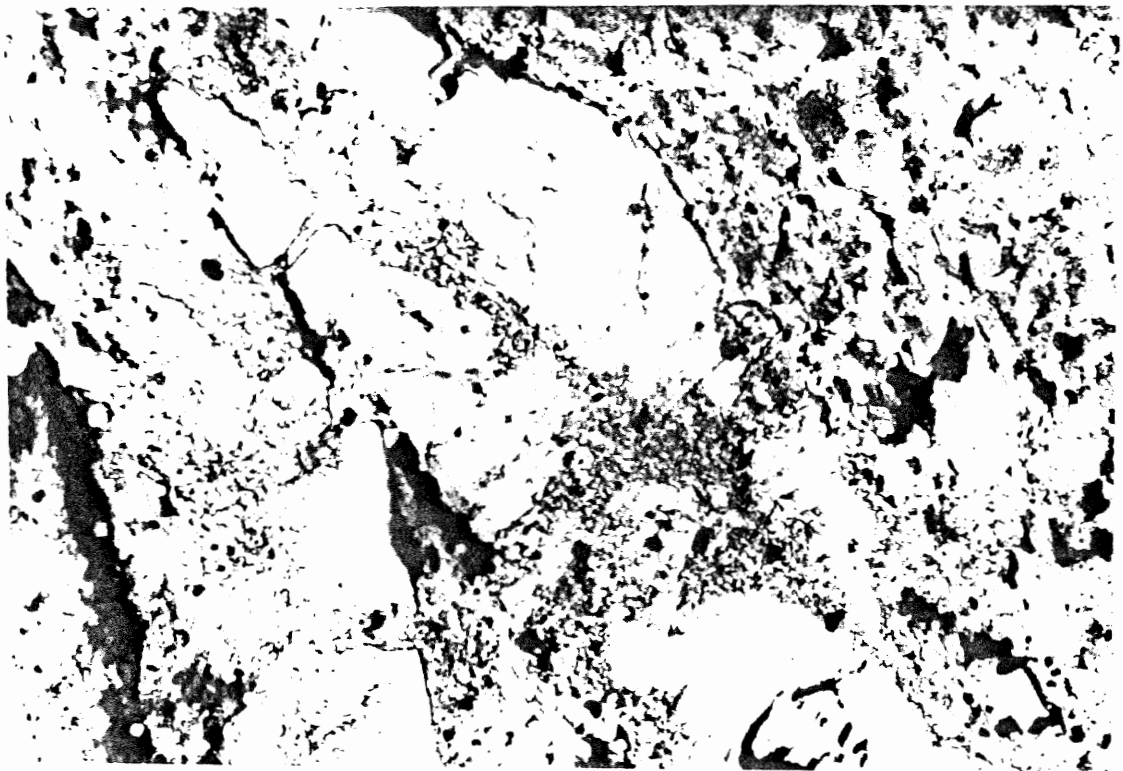


Fig 3.4 Andalusite porphyroblasts and biotite in BB-97-10. Field of view is 1 x 2 mm.

muscovite and biotite (fig. 3.6). Regional fabric (S1) in group 4 samples is defined by parallel alignment of sulphides (fig. 3.7). The psammitic composition of group 4 samples is reflected by the absence of silicate porphyroblasts and is represented by samples BB-97-11, BB-97-21, and BB-97-22. Sample BB-97-11 contains 15% elongate subidioblastic to xenoblastic pyrite porphyroblasts up to 6 mm long with minor chalcopyrite. Samples BB-97-21 and BB-97-22 have medium-grained, equant quartz with sericite. Sample BB-97-21 includes muscovite, biotite, and minor sulphides, while sample BB-97-22 has chlorite veins but no well defined regional fabric.

Group 5 samples occur 470-1270 m from the contact of the SMB and show a parallel alignment of elongate sulphide grains (fig. 3.8). Group 5 includes samples with porphyroblasts of pyrrhotite (+/- cordierite), and is represented by samples BB-97-3, BB-97-7, and BB-97-13. Sample BB-97-3 contains 15% subidioblastic to xenoblastic pyrrhotite porphyroblasts up to 6 mm long with minor inclusions of chalcopyrite. The elongate crystals are parallel and have inclusions of quartz, muscovite, and biotite. One large porphyroblast includes elongate clusters of pyrite spheres in pyrrhotite, giving a vermicular appearance (fig. 3.9). Sample BB-97-7 contains 20% cordierite porphyroblasts 2 mm in diameter, and 10% subidioblastic to xenoblastic pyrrhotite porphyroblasts with intergrown ilmenite forming rims, with fine-grained pyrite and minor chalcopyrite in the groundmass (fig. 3.10). Sample BB-97-13 contains 10% altered cordierite porphyroblasts and 20% pyrrhotite defining a lineation at 086° . Pyrrhotite porphyroblasts are aligned parallel to cordierite porphyroblasts and define a foliation which is subparallel to bedding ($282^{\circ}/54^{\circ}$).

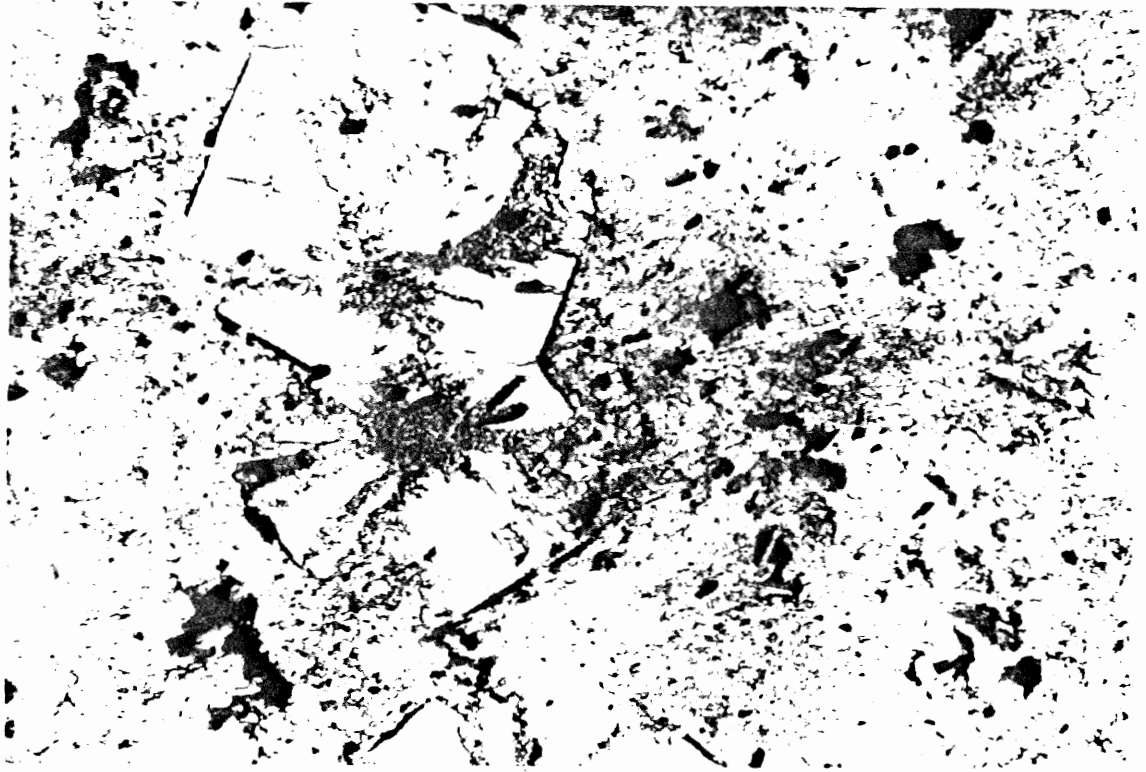


Fig. 3.5 Andalusite and cordierite in sample BB-97-2. Field of view is 1 x 2 mm.

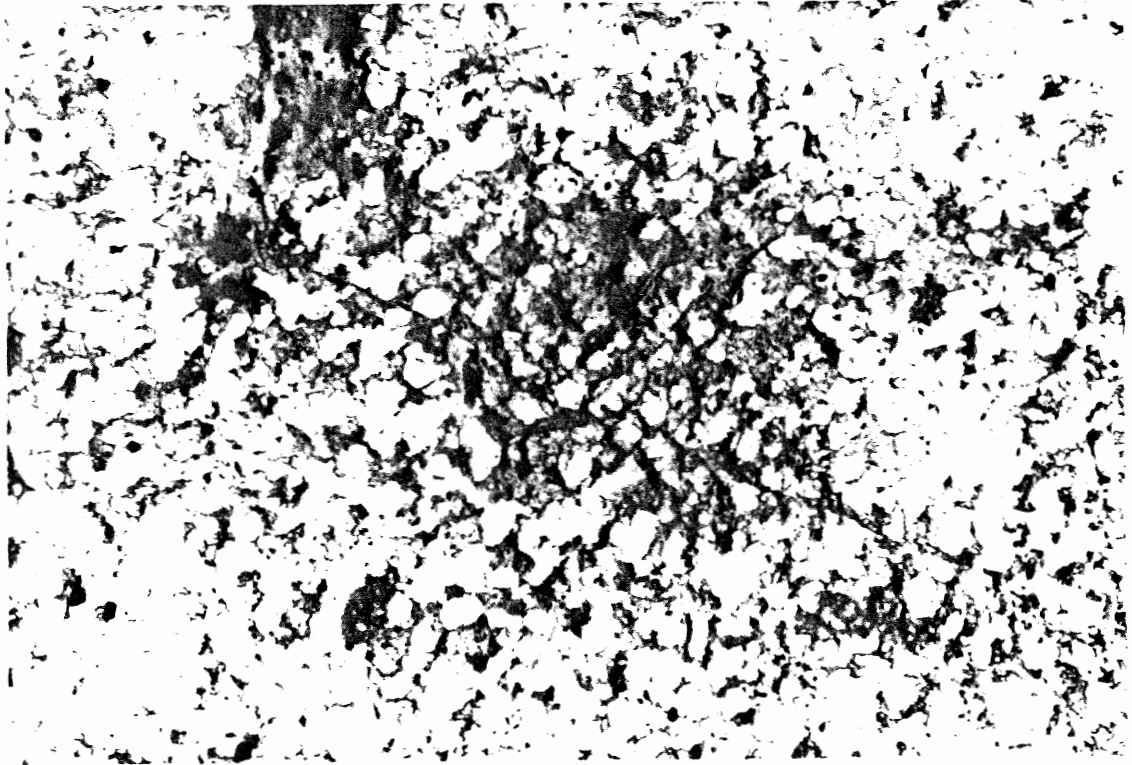


Fig. 3.6 Quartz rich lithology of group 4. Field of view is 1 x 2 mm.

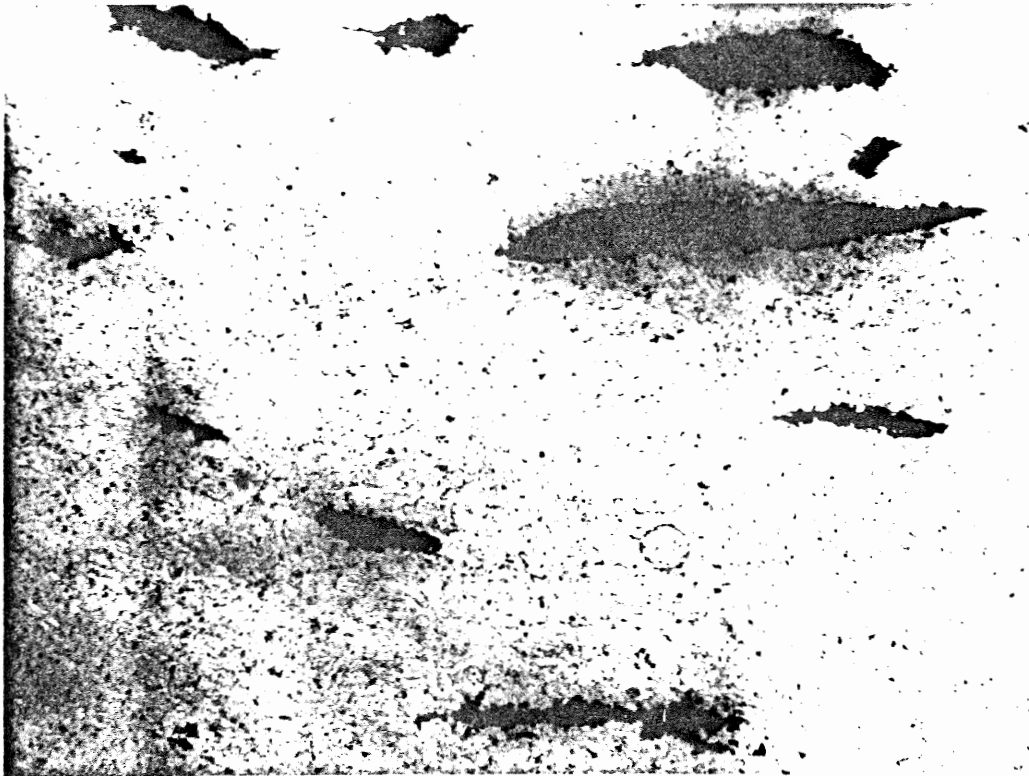


Fig. 3.7 Parallel alignment of sulphides defining S1 in group 4 samples. Field of view 10 x 14 mm.

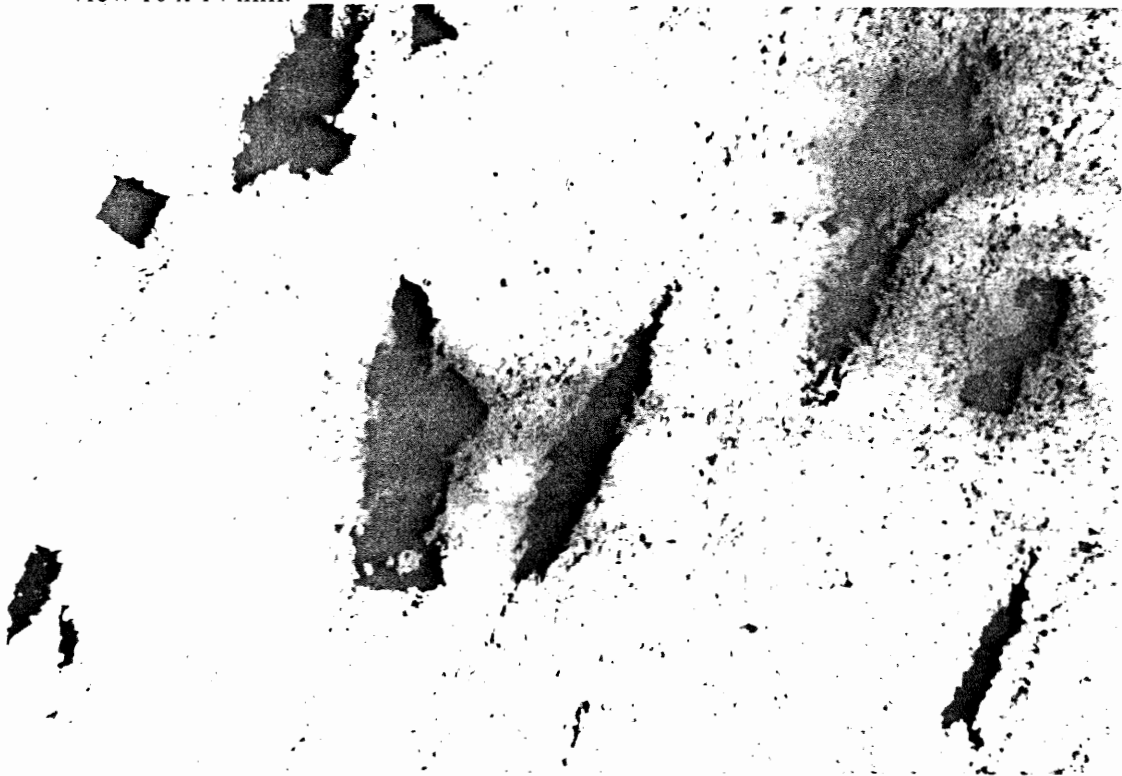


Fig. 3.8 Parallel alignment of elongate sulphides in group 5 samples. Field of view is 10 x 14 mm.

Group 6 is represented by sample BB-97-6 which occurs 860 m from the contact of the SMB, and includes porphyroblasts of andalusite and cordierite (fig. 3.11). This sample is in its own group because andalusite does not occur in other samples more than 620 m from the contact. This sample contains 30% subidioblastic andalusite porphyroblasts up to 3 mm across which are rimmed by graphite and 20% idioblastic cordierite porphyroblasts up to 0.5 mm in diameter. Sample BB-97-6 also includes minor pyrite in the groundmass.

3.3 Mineral Chemistry

Microprobe analyses (Appendix C) were performed on five samples representative of the study area. Both sulphides and silicates were analyzed and show consistent results with distance from the contact. A plot of percent iron versus distance shows the relatively constant iron content of sulphides and silicates (several grains averaged per sample) from samples throughout the contact aureole (fig. 3.12). Slight changes in iron content are within the margin of error.

Groups are based primarily on silicate mineral assemblages, and show a definite relationship to distance from the contact, as shown from a plot of samples according to group against distance from the contact (fig. 3.13).

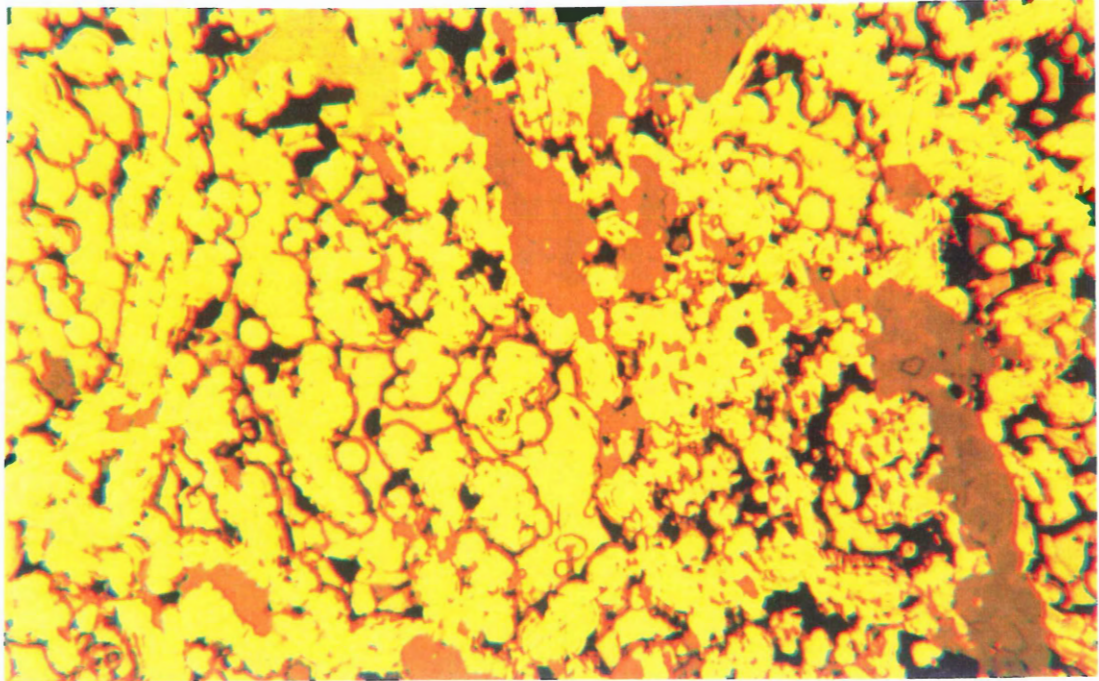


Fig. 3.9 Pyrite spheres in pyrrhotite from sample BB-97-3. Field of view is 1 x 2 mm.

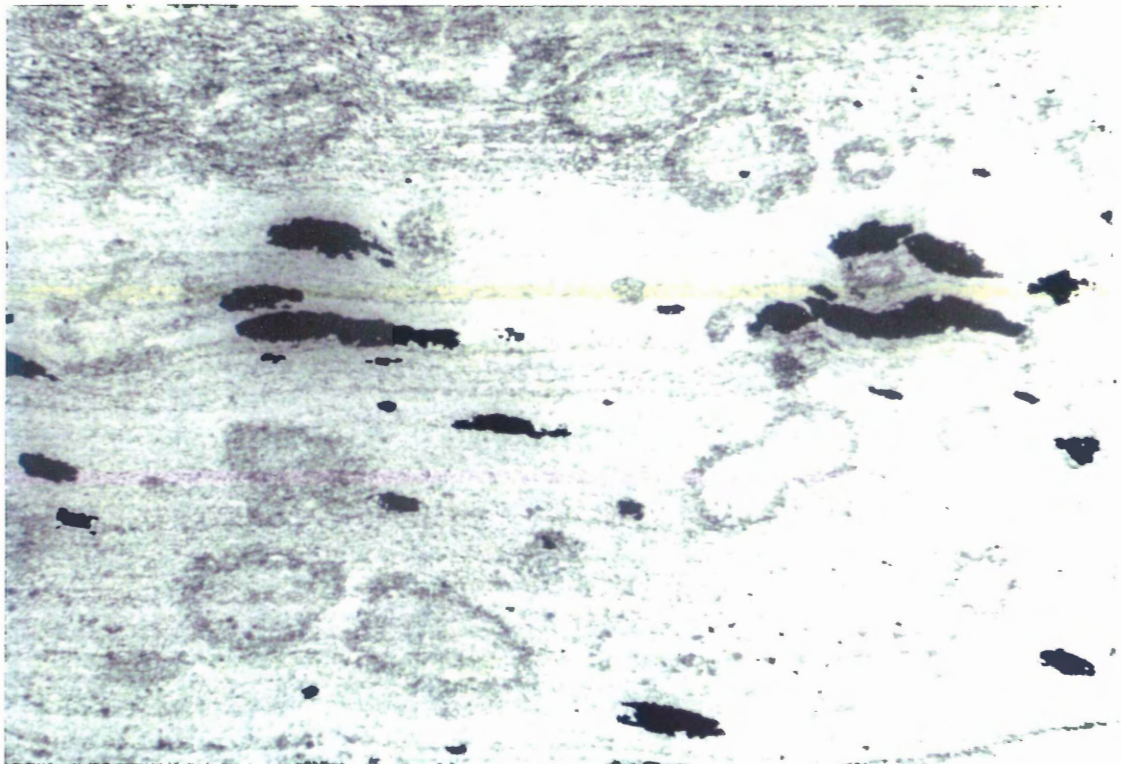


Fig. 3.10 Cordierite and pyrrhotite porphyroblasts from sample BB-87-7. Note fabric and pyrrhotite wrapping around cordierite. Field of view is 10 x 14 mm.



Fig. 3.11 Porphyroblasts of andalusite and cordierite from sample BB-97-6 at 860 m from the contact. Field of view is 1 x 2 mm.

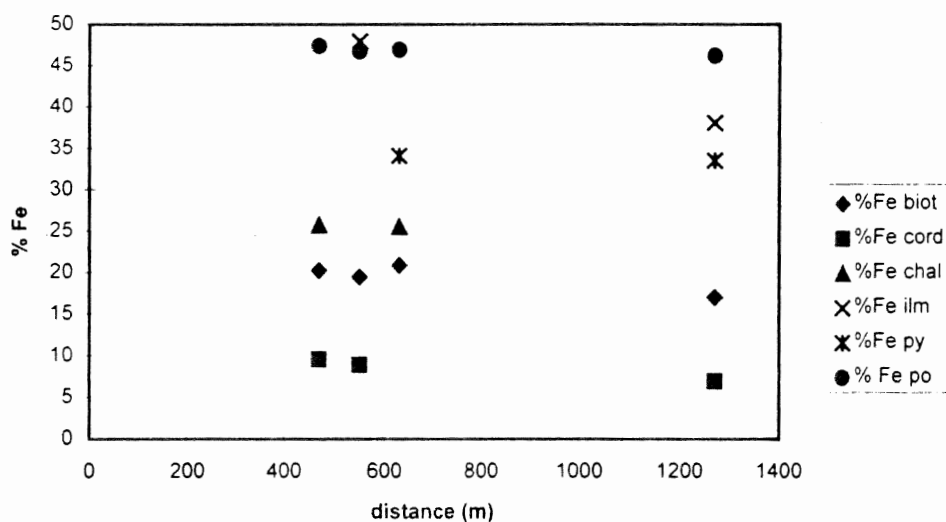


Fig. 3.12 Plot of percent iron from sulphides and silicates against distance from the contact of the SMB. This plot shows that iron content does not change dramatically with distance from the contact. Data points represent sample averages from several grains. Biot = biotite, cord = cordierite, chal = chalcopyrite, ilm = ilmenite, py = pyrite, po = pyrrhotite.

3.3.1 Sulphide Mineral Assemblage and Grain Size

A plot of modal percent total sulphides versus distance (fig. 3.14) shows no pattern of sulphide abundance with distance from the contact. There is also no pattern observed when modal percent sulphide by type (pyrrhotite-pyrite) versus distance is plotted (fig. 3.15). The grain size of sulphides versus distance from the contact was also plotted (fig. 3.16). Pyrite coarsens toward the contact but pyrrhotite shows no distinct pattern with distance from the contact. Pyrrhotite is monoclinic away from the contact and hexagonal close to the contact, determined by increasing iron content.

3.3.2 Silicate Mineral Assemblage

A plot of modal percent silicate minerals versus distance from the contact shows a transition from cordierite to andalusite through sillimanite, toward the contact (fig. 3.17). Four distinct fields can be identified which illustrate a progressive change in mineral assemblage. These include a cordierite field from the outer limits of the study area; an andalusite plus cordierite field at 380-860 m from the contact; an andalusite field from 200-380 m from the contact; and a sillimanite (fibrolite) plus andalusite field which extends 200 m from the contact (Table 3.2).

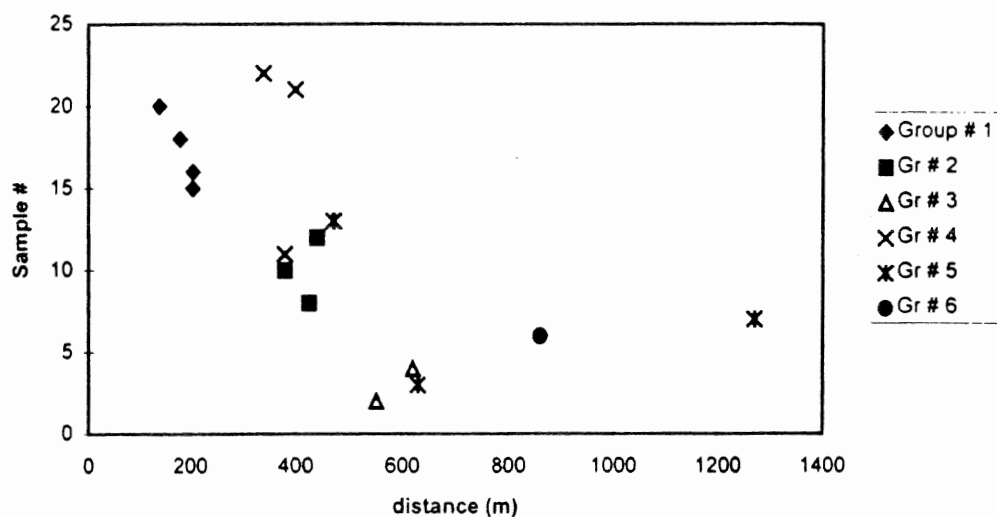


Fig. 3.13 Plot of samples by group with distance from the contact of the SMB. Groups are based on silicate porphyroblasts, and reflect the thermal effect of contact metamorphism.

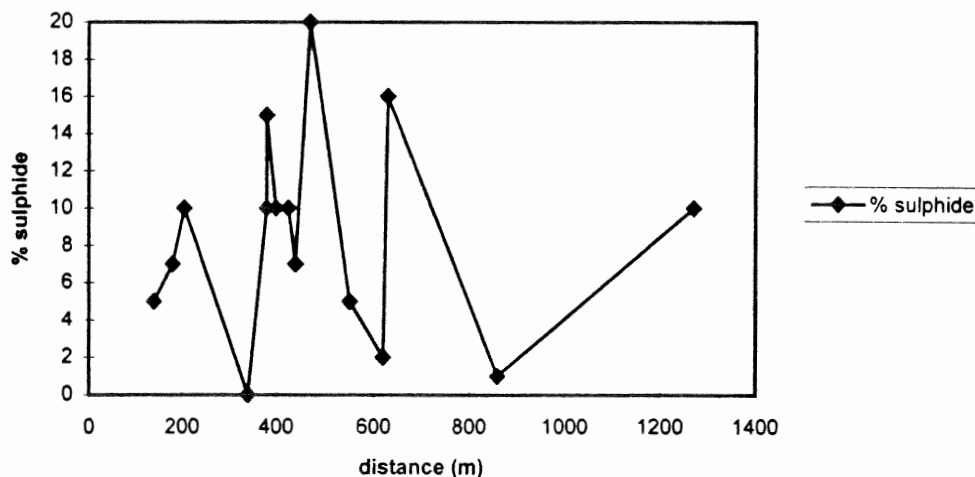


Fig. 3.14 Plot of modal percent total sulphides versus distance from the contact. There is no pattern of sulphide abundance with distance from the contact.

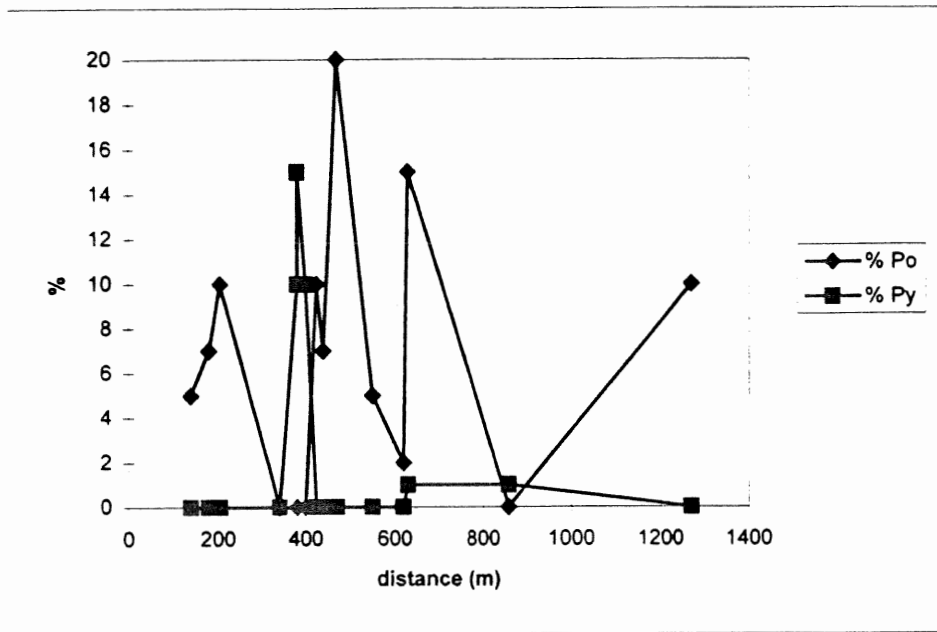


Fig. 3.15 Plot of modal percent sulphide by type versus distance from the contact. There is no pattern of pyrite or pyrrhotite abundance with distance from the contact. Po = pyrrhotite, py = pyrite.

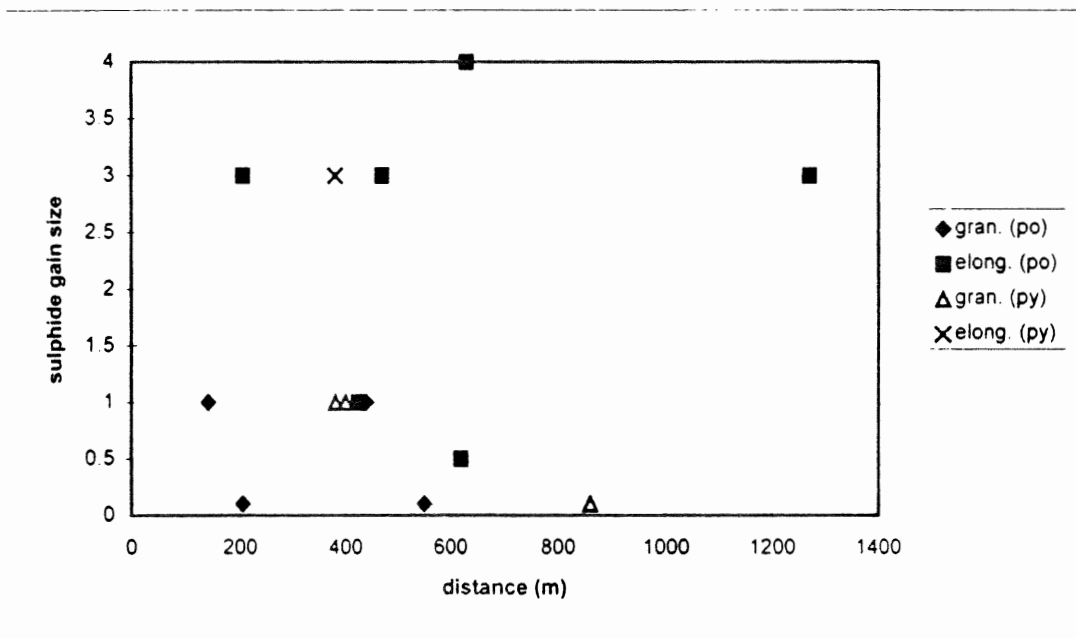


Fig. 3.16 Sulphide grain size (mm) versus distance from the contact. Different symbols are used to indicate elongate and equant grains. This plot shows that pyrite coarsens toward the contact but pyrrhotite shows no distinct pattern with distance from the contact. Po = pyrrhotite, py = pyrite, gran = equant grains, elong = elongate crystals.

Table 3.2 Silicate mineral assemblage fields with distance from the contact of the SMB

Field 1	Field 2	Field 3	Field 4
sillimanite + andalusite	andalusite	andalusite + cordierite	cordierite
perthite		k-feldspar	
biotite + muscovite	biotite + muscovite	biotite + muscovite	biotite + muscovite
0-200 m	200-380 m	380-860 m	860-1270 m

3.4 Generalized Silicate and Sulphide Relationships

Group 5 samples span a wide range of distances from the contact (470-1270 m) and show variable amounts of pyrrhotite and cordierite. Group 6 is represented by sample BB-97-6 at 860 m from the contact. Regional cleavage is well developed in this sample. Group 4 samples occur 340-400 m from the contact, and there is no (S1) fabric. Group 4 represents a more quartz-rich lithology and is coarse-grained relative to other samples. Group 3 samples include fine-grained sulphides (<5%) with andalusite and cordierite at 550-620 m. Regional cleavage (S1) is poorly developed in group 3 samples. Sulphides in Group 2 samples are medium-grained and occur with both andalusite and cordierite at 380-450 m. Parallel elongate grains define a foliation in group 2 samples. Group 1 samples include fibrolite, are closest to the contact (0-200 m), and have minor fine-grained sulphides. Regional cleavage (S1) is annealed. These relationships can be seen in Table 3.2, which summarizes mineralogy with respect to distance from the contact.

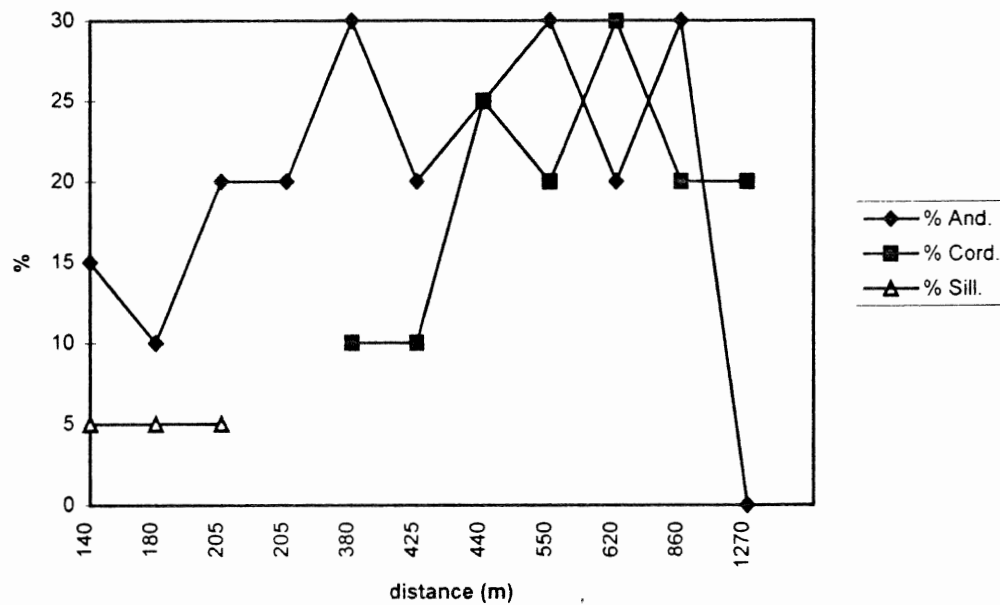


Fig. 3.17 Plot of modal percent silicate porphyroblasts versus distance from the contact. This shows four distinct fields from cordierite to cordierite + andalusite to andalusite to andalusite + sillimanite (fibrolite) toward the contact. And = andalusite, cord = cordierite, sill = sillimanite.

Microprobe results were plotted on a standard AFM diagram (fig. 3.18). The iron content ($\text{Fe}/\text{Fe} + \text{Mg}$) of silicates increases with increasing contact metamorphic grade (not indicated in the plot of percent iron versus distance shown in fig. 3.12). Sulphide variety was included on the diagram and shows that hexagonal pyrrhotite is associated with highest grade samples.

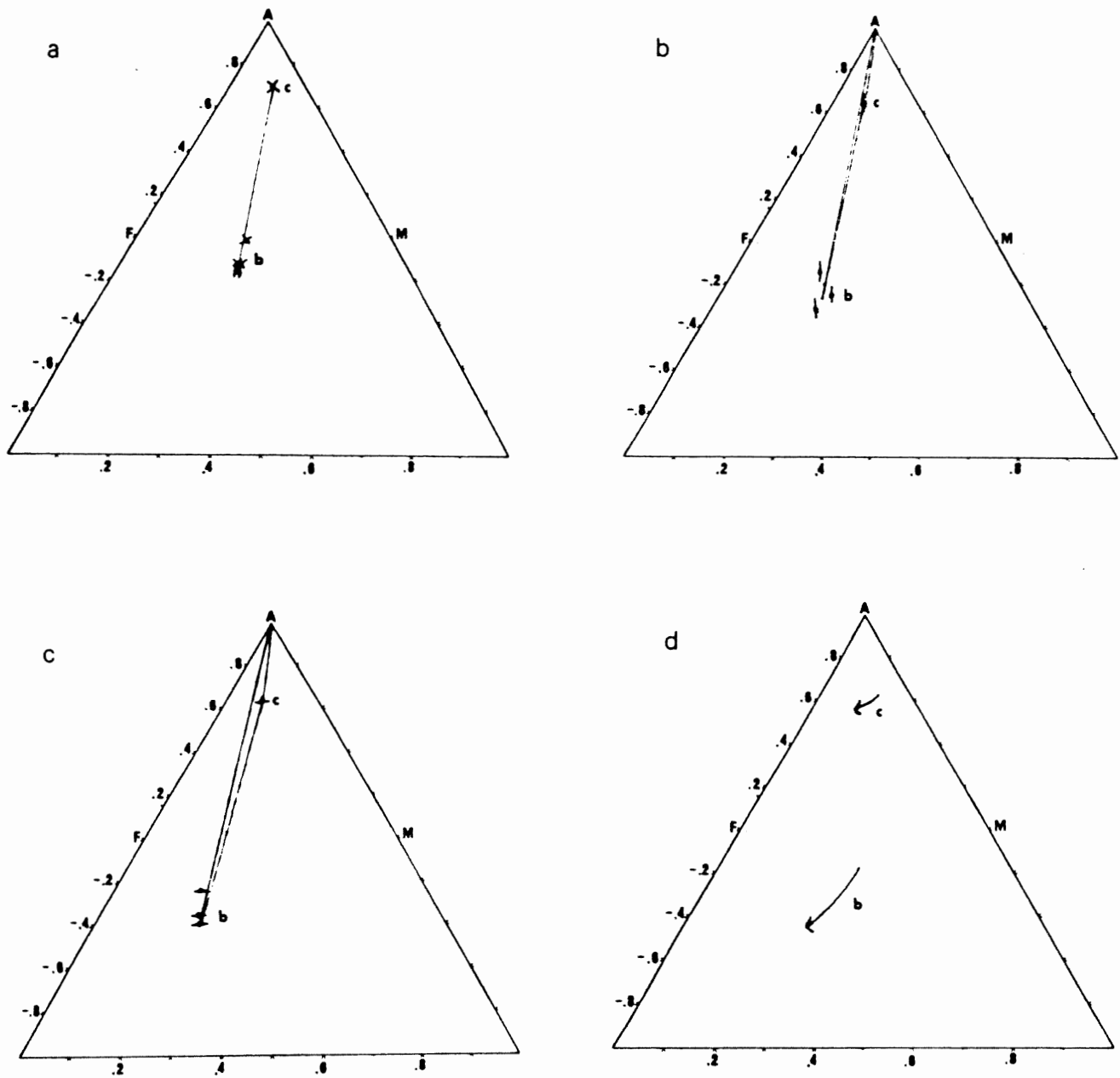


Fig. 3.18 AFM diagram plotting cordierite (c.), biotite (b) and andalusite compositions from microprobe analyses, a.) shows analyses for sample BB-97-7. Sulphides present include pyrite and monoclinic pyrrhotite which occur in different beds. b.) shows analyses for sample BB-97-2 which includes monoclinic pyrrhotite. c.) shows analyses for sample BB-97-5b which includes hexagonal pyrrhotite. d.) shows the general trends of the analyses. Iron content ($\text{Fe}/\text{Fe} + \text{Mg}$) of both cordierite and biotite increase with increasing metamorphic grade (BB-97-7 to BB-97-2 to BB-97-5b). Hexagonal pyrrhotite occurs only in highest grade sample.

Table3.3 Sample data ordered by distance from the contact with the South Mountain Batholith,

Sample #	Distance (m)	P'blasts	Texture	% And. (*fibrolite present)	% Cord.	% Po	% Py	Group #
BB-97-20	140	and.	Fine-grained	15 *	0	5	0	1
BB-97-18	180	and.	Fine Hornfels	10 *	0	7	0	1
BB-97-15	205	and.	Fine Hornfels	20 *	0	10	0	1
BB-97-16	205	and.	Fine	20	0	10	0	1
BB-97-22	340	NA	medium	0	0	0	0	4
BB-97-10	380	and., cord. & biot.	Hornfels Elongate and. Parallel 187°	30	10	0	10	2
BB-97-11	380	py	elongate grains parallel	0	0	0	15	4
BB-97-21	400	NA	medium	0	0	0	0	4
BB-97-8	425	and., cord. & biot.	Hornfels Fabric parallel 170°	20	10	10	0	2
BB-97-12	440	and., cord. & biot.	Elongate grains parallel Hornfels	25	25	7	0	2
BB-97-13	470	cord. & po	Hornfels fabric parallel 086°	0	10	30	0	5
BB-97-2	550	and., cord., & biot.	fine	30	20	5	0	3
BB-97-4	620	and., cord. & biot.	fine	20	30	2	0	3
BB-97-3	630	po	elongate grains parallel	0	0	15	0	5
BB-97-6	860	and., cord. & biot.	Fabric deflects around and.?	30	20	0	<1	6
BB-97-7	1270	cord & po	fabric parallel 238°	0	20	10	0	5

** po = pyrrhotite cord = cordierite biot = biotite
 py = pyrite and = andalusite p'blasts = porphyroblasts

CHAPTER 4

Interpretations and Discussion

4.1 Introduction

The objectives of this study include determination of the relationship between porphyroblast growth and fabric development in the study area, documentation of changes in sulphide mineralogy with distance from the contact of the SMB, and correlation between changes in sulphide and silicate mineralogy with distance from the contact. The following is a discussion of data relevant to these objectives.

4.2 Porphyroblast Growth and Fabric Development

To determine the relationship between porphyroblast growth and fabric development the temporal sequence of metamorphism was identified through petrographic analysis.

Low grade regional metamorphism at 395-388 Ma (Hicks *et al.*, submitted) produced cleavage which constitutes the dominant fabric (S1) observed within the contact aureole of the SMB. In the outer part of the contact aureole, biotite grains are aligned parallel to cleavage (S1) (fig. 4.1).

Cordierite crystallization occurred after biotite growth and (S1) cleavage development, as interpreted from cordierite inclusions (biotite and opaque minerals)

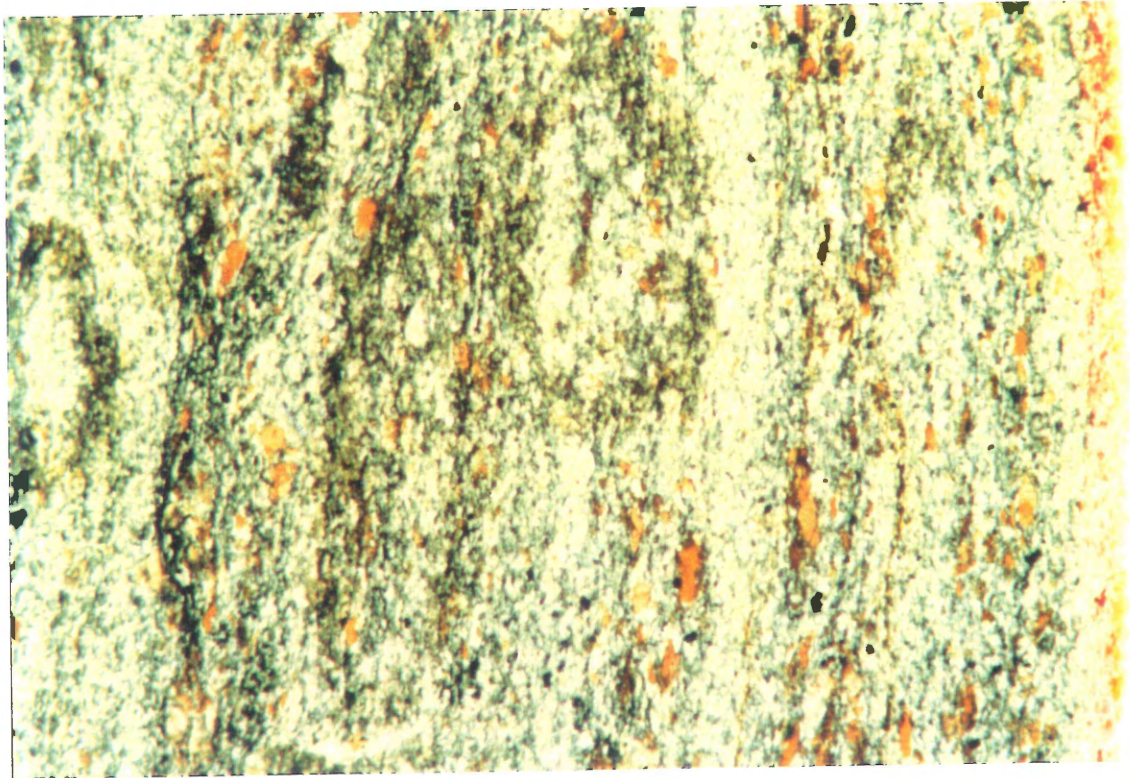


Fig. 4.1 Biotite grains parallel regional cleavage (S1). Field of view is 2 x 4 mm.

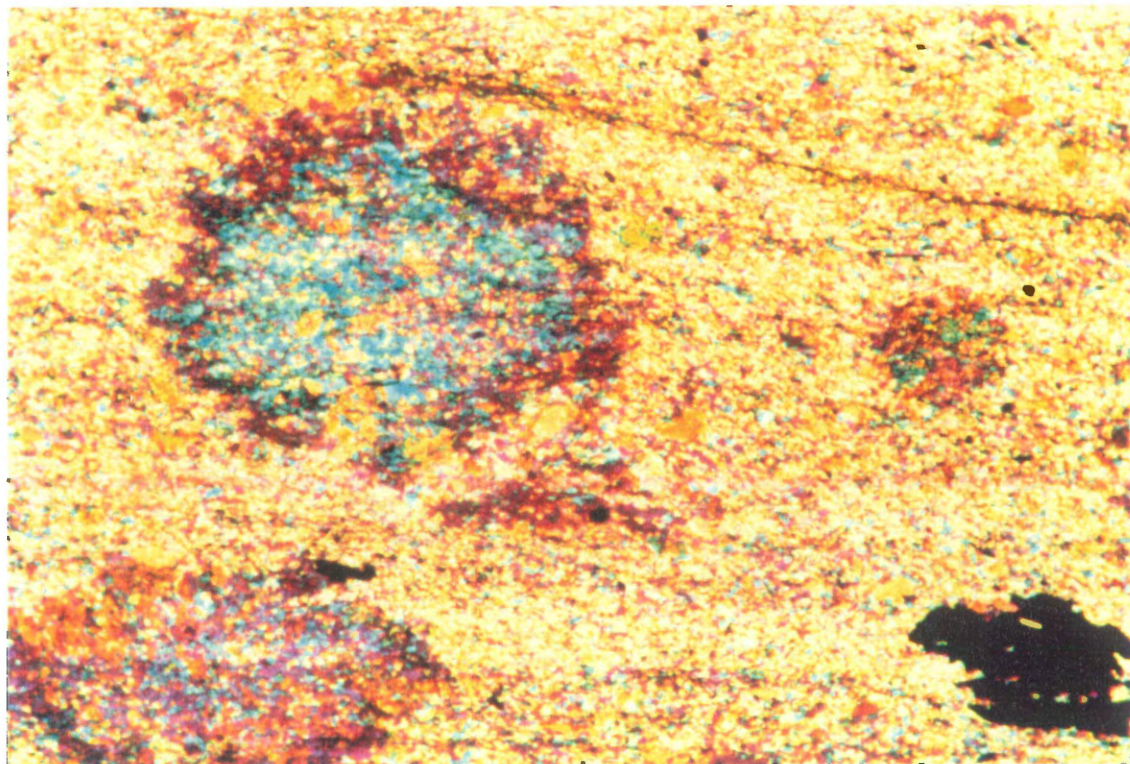


Fig. 4.2 Inclusions in cordierite parallel cleavage. Field of view is 2 x 4 mm.

parallel to cleavage (fig. 4.2). The timing of sulphide growth is uncertain from textural relationships: it may be syn-cordierite growth, or it may pre-date fabric development (S1). Field observation of sulphides stretched along cleavage (S1) planes suggests pre-cleavage sulphide growth. However, sulphides may be syn-regional cleavage (S1) and pre-fabric deflection (S2), but this cannot be determined from textural relationships in the present sample set (see study by Pradeep Bhatnagar, 1998).

Reactivation of the regional cleavage (S1) occurred after cordierite and sulphide growth. As a result, the regional fabric is deflected (S2) around cordierite grains, and biotite and sulphides are also deflected around cordierite (fig. 4.3).

Andalusite crystallization occurred after cordierite growth, as andalusite crystals grow across cordierite (fig. 4.4). Andalusite also grew after deflection of the regional fabric (S1). This is determined from andalusite growth parallel and perpendicular to the regional fabric (fig. 4.5), which shows that S2 fabric did not reorient andalusite porphyroblasts. Deflection (S2) of the regional fabric around andalusite is common, but does not always occur and where there is deflection, a cordierite grain is usually associated with S2 (fig. 4.6). This relationship suggests that the apparent deflection of regional fabric around the andalusite is actually a deflection of fabric around cordierite.

Finally, retrogression of cordierite produced biotite and muscovite randomly oriented relative to both S1 and S2 fabrics (fig. 4.7). This temporal sequence is illustrated in figure 4.8.

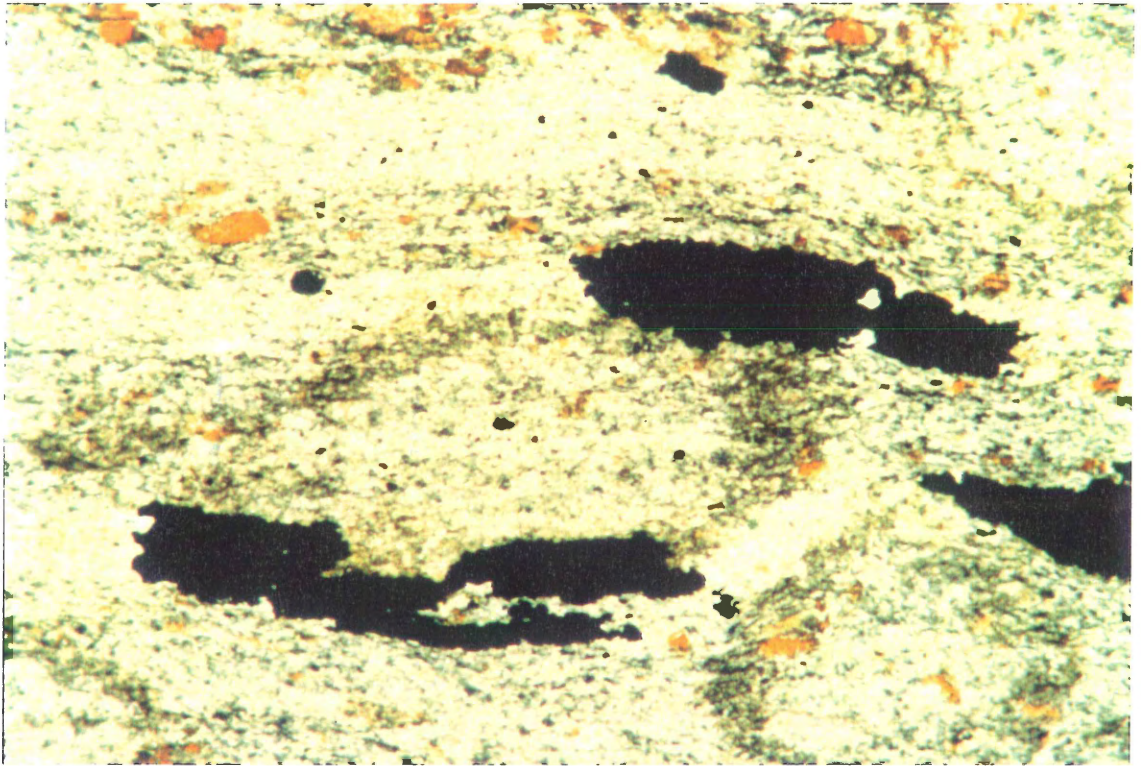


Fig. 4.3 Biotite and sulphides deflected around cordierite. Field of view is 2 x 4 mm.

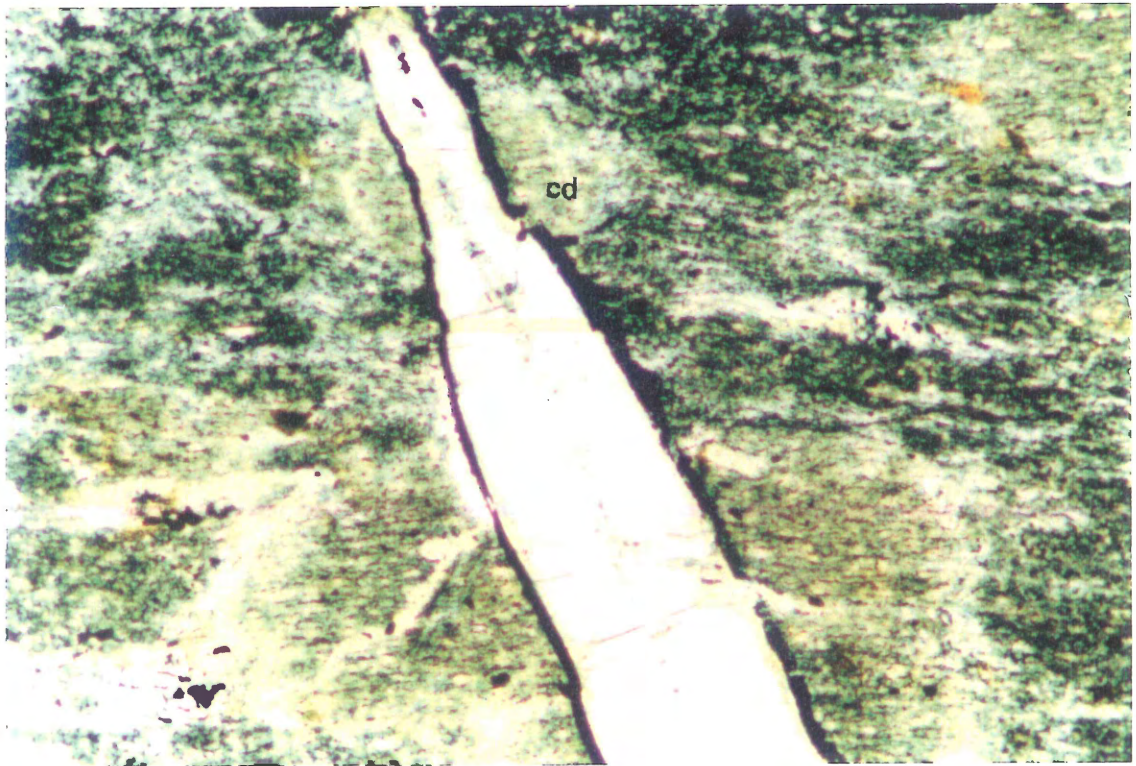


Fig. 4.4 Andalusite crystal growing across cordierite (cd). Field of view is 1 x 2 mm.



Fig. 4.5 Andalusite growing parallel and perpendicular to regional fabric (S1). Field of view is 3 x 5 mm.

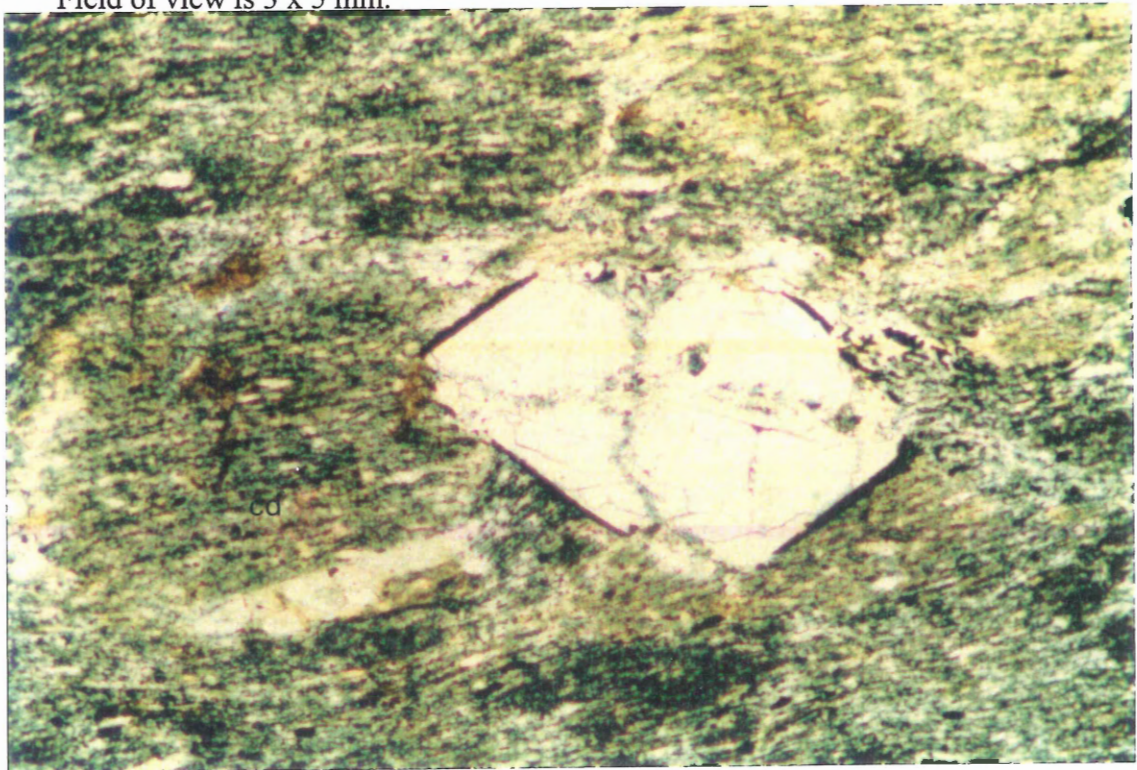


Fig. 4.6 S2 fabric deflected around cordierite (cd) into andalusite. Field of view is 1 x 2 mm.

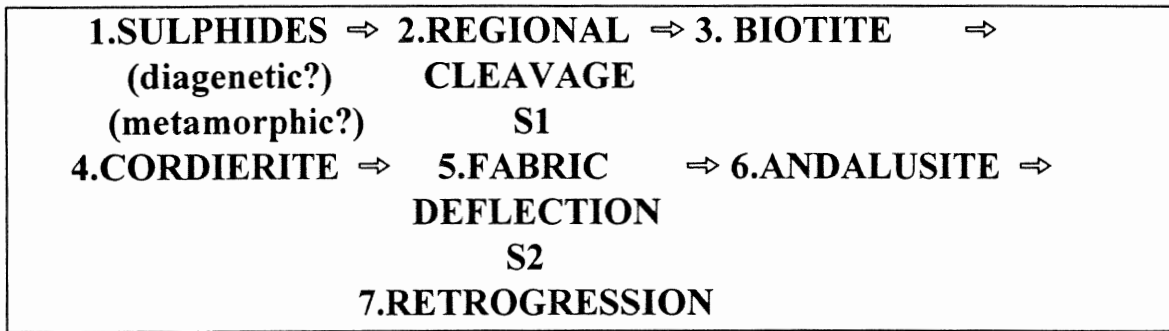


Fig. 4.8 Temporal sequence of metamorphism in Halifax Group rocks of the contact aureole of the South Mountain Batholith, as determined through petrographic analysis.

This temporal sequence of fabric development and porphyroblast growth is based on relationships in samples at the greatest distance from the contact, where early regional fabrics (S1) are preserved. Nearer the contact of the SMB regional cleavage (S1) is annealed, and fabric-porphyroblast relationships cannot be determined.

4.3 Changes in Mineralogy with Distance from the Contact

Pyrrhotite and pyrite are the dominant sulphide minerals in the contact aureole of the SMB and in the Meguma Supergroup (Robinson, 1996; Jones, 1997). In general these two sulphide phases do not occur together as porphyroblasts. Data presented suggest that sulphide occurrence has a lithological rather than thermal control. In particular, sulphide abundance shows no relationship with distance from the contact. Pyrite coarsens toward the contact but pyrrhotite shows no pattern in size with distance from the contact. This suggests that temperature has little effect on sulphide grain size.

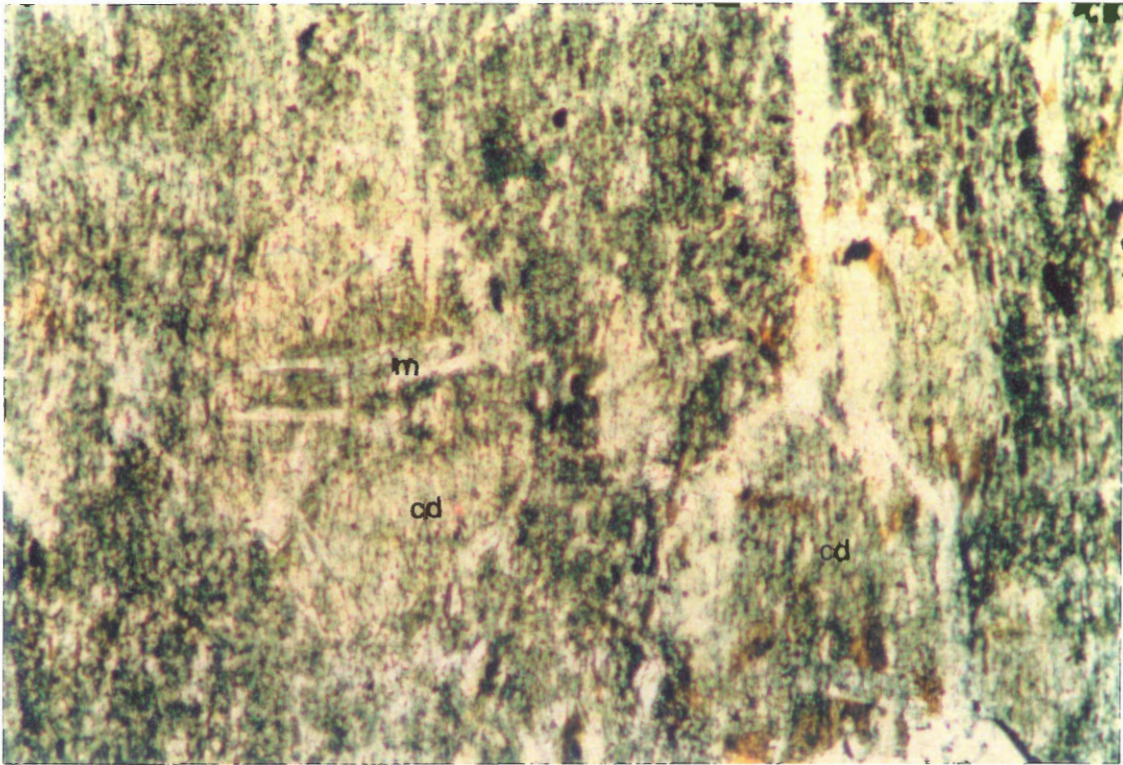


Fig. 4.7 Randomly oriented mica (m = muscovite, b = biotite) inside cordierite (cd) grains. Field of view is 1 x 2 mm.

Contact metamorphism may have affected pyrrhotite. Pyrrhotite ranges from monoclinic to hexagonal, and hexagonal pyrrhotite occurs in higher grade samples (fig. 3.18).

Silicate mineralogy changes systematically with distance from the contact of the SMB. This systematic change, documented in figure 3.17, suggests that silicate mineral assemblage reflects the thermal effect associated with contact metamorphism. Cordierite and biotite are abundant from the outer limits of the study area up to approximately 400 m from the contact. As metamorphic grade increases cordierite is more altered.

Andalusite first appears at 860 m from the contact and persists to the contact. In samples within 200 m of the contact, sillimanite begins to appear as fibrolite. Fibrolite is seen growing around and between andalusite grains, as well as in association with biotite. K-feldspar was analyzed from sample BB-97-2 at 550 m from the contact.

The succession from cordierite to andalusite to sillimanite is typical of contact aureoles in pelitic rocks (eg. the Ballachulish aureole, Scotland; Pattison and Tracy, 1991). Mahoney (1996) documented this succession in the contact aureole of the SMB in Halifax Group rocks from around the batholith.

Microprobe data of silicate and sulphide iron contents suggest that contact metamorphism did not strongly affect the sulphide phases present in the country rocks. This finding is somewhat contradictory to findings presented in the literature (Mohr and Newton, 1983; Tracy and Robinson, 1988) which suggest that during metamorphism pyrite is converted to pyrrhotite and silicates become depleted in iron. In the present study, as contact metamorphic grade is increased, there is no systematic change in sulphide mineral assemblage and silicate iron content increases only slightly (fig. 3.18). Sulphur fugacity is also considered a controlling factor in determining silicate iron

contents in the presence of sulphides (Hutcheon, 1979), but this cannot be tested with the data available in this study.

While it is clear that the origin and distribution of silicates such as sillimanite, andalusite, and cordierite are thermally controlled in the contact aureole of the SMB, the origin and distribution controls of sulphides are not so easily determined. Country rock lithology is the most obvious control on sulphide distribution, from petrological, chemical, and field data. Sulphide origins cannot be determined directly from the available data of this study, but hypotheses can be made.

The preferential occurrence of the sulphides in organic-rich slates suggests a diagenetic origin for regional pyrrhotite and pyrite. An Early Ordovician anoxic event (Schenk, 1991) could provide the reducing environment necessary to precipitate sulphides (Waldron, 1987) in black shales (i.e. the Cunard Formation). Regional pyrrhotite could be easily formed by a release of sulphur from pyrite. Textural relationships between pyrrhotite and pyrite determined petrographically (fig. 3.9) indicate that the two formed at approximately the same time.

The temporal relationship between sulphides and fabric (S1 & S2) development is unclear, but sulphides may have formed syn-S1 fabric, during low grade regional metamorphism. It can be stated with certainty that sulphides pre-date the development of S2, which could be related to the emplacement of the SMB. Under these conditions, sulphides formed during low grade regional metamorphism but were not chemically affected by contact metamorphism.

4.4 Pressure-Temperature Conditions

The contact aureole of SMB was documented by Mahoney (1996). She concluded that the width of the contact aureole around the SMB varies significantly, and is widest where highest pressures were recorded. The aureole in the Halifax area is among the widest, where P-T conditions of 3.7 ± 0.2 Kbar and $520 \pm 40^\circ\text{C}$ were calculated.

The P-T conditions for emplacement of the Halifax pluton, in the study area, of the SMB are estimated here using a P-T diagram from Pattison and Tracy (1991). From this diagram (fig 4.9) a maximum pressure of approximately 3.0 Kbar is determined. This estimate is significantly lower than that calculated by Mahoney (1996). The maximum temperature estimated from Pattison and Tracy's (1991) diagram is between 590°C and 620°C . This estimate is also quite different from that calculated by Mahoney (1996).

The presence of andalusite and K-feldspar suggests lower pressure in the contact aureole than calculated by Mahoney (1996), however, a direct comparison using techniques applied by Mahoney (1996) are not possible with the microprobe data and mineral assemblages in the present study.

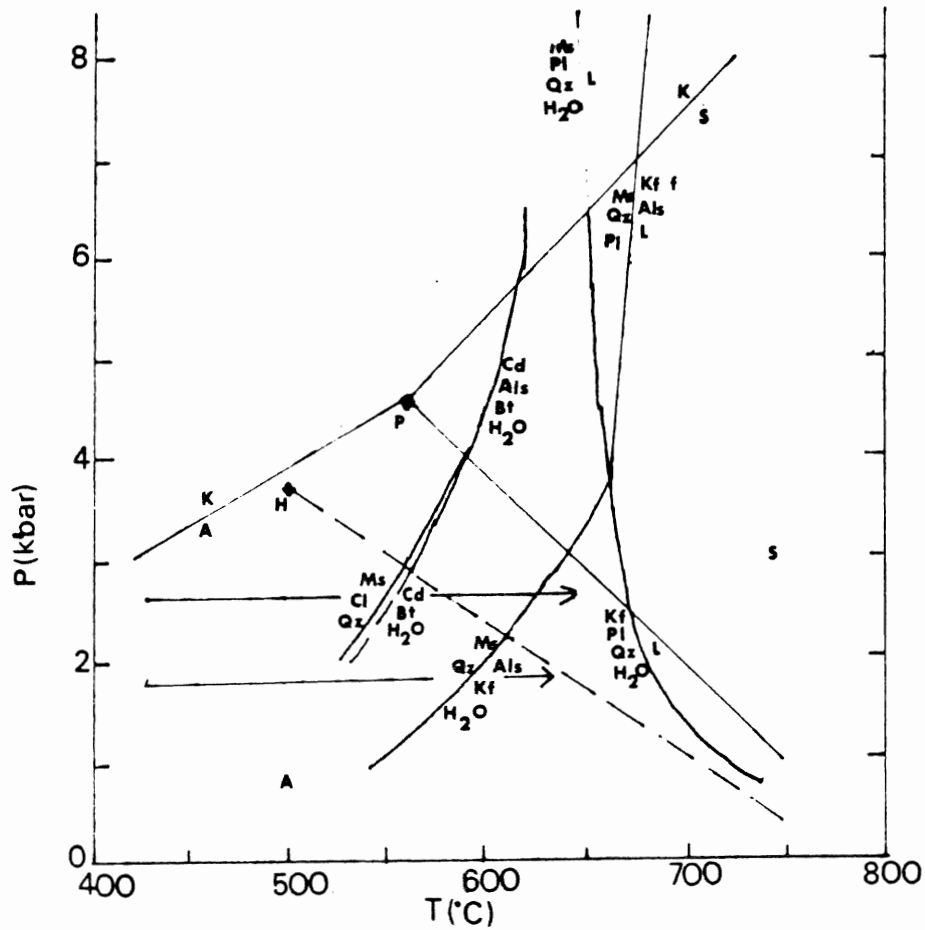


Fig. 4.9 P-T diagram showing kyanite-andalusite-sillimanite fields plus reactions relevant to the mineral assemblages of samples in the present study. Both Pattison (P) and Holdaway (H) triple points are shown. Arrows (one for each triple point) indicate temperature path from the country rocks toward the contact assuming constant pressure. From this diagram a maximum pressure of 3.0 kbar and a maximum temperature between 590°C and 620°C are estimated. Diagram modified from Pattison and Tracy, 1991.

CHAPTER 5

Conclusions

5.1 Conclusions

Petrographic evidence presented in this study indicates that the silicate mineral assemblage of Halifax Group rocks in the contact aureole of the SMB varies systematically with distance from the contact in rocks of similar composition, and is therefore thermally controlled. The thermal energy was provided by the cooling SMB, and is thus described as a contact metamorphic effect.

Petrographic, mineral chemistry, and field data presented in this study indicate that the sulphide mineral assemblage of Halifax Group rocks in the contact aureole of the SMB is lithologically controlled. It is therefore concluded that sulphide mineral assemblage has no direct relationship to contact metamorphism.

Petrographic and field data have been used to develop a temporal sequence of events in the contact aureole of the SMB to better understand silicate-sulphide-fabric relationships. 1. Sulphide growth (diagenetic or low-grade metamorphic), 2. regional cleavage (S1), 3. regional biotite, 4. cordierite growth, 5. deflection of regional cleavage around cordierite (S2), 6. andalusite growth, 7. retrogression of cordierite.

In conclusion, the complicated relationships of porphyroblasts and fabrics in the contact aureole of the SMB result from thermal effects superimposed on lithological differences. Halifax Group lithological variations give rise to different sulphide

assemblages. Silicate porphyroblasts resulted from contact metamorphism of Halifax Group rocks by the SMB. Regional cleavage (S1) is primarily the product of regional low-grade metamorphism, and the later reactivation of fabric (S2) is an emplacement effect (S2 occurred between cordierite and andalusite growth).

5.2 Future Work

Future work in Halifax Group rocks in the contact aureole of the SMB should include a systematic geochemical study of sulphides and country rocks to better understand the relationship of sulphide mineralogy to rock type. This would have both academic as well as practical applications, eg. the problem of acid rock drainage (ARD).

Future work may also include extending the present study farther into the country rocks to find the biotite isograd. Isograd mapping in the aureole would be an excellent supplement to current data from the contact aureole. Determining the distribution of K-feldspar in the aureole would improve current estimates of P-T conditions.

The presence of bitumen in samples of this study was noted by Nick Wilson, and this should be examined by future workers.

REFERENCES

- Abbott, R.N. 1989. Internal structures in part of the South Mountain Batholith, Nova Scotia, Canada. *Geological Society of America Bulletin*, **101**: 1493-1506.
- Benn, K., Horne, R.J., Kontak, D.J., Pignotta, G.S., Evans, N.G. 1997. Syn-Acadian emplacement model for the South Mountain Batholith, Meguma Terrane, Nova Scotia: magnetic fabric and structural analyses. *Geological Society of America Bulletin*, **109**: 1279-1293.
- Charest, M.H., Farley, E.J., and Clarke, D.B. 1985. The northwestern part of the New Ross-Vaughn Complex: petrology, geochemistry and mineral deposits. *In: Guide to the Granites and Mineral Deposits of Southwestern Nova Scotia. Edited by A.K. Chatterjee and D.B. Clarke. Nova Scotia Department of Mines and Energy, Paper 85-3: 29-40.*
- Clarke, D.B. and Meucke, G.K. 1985. Review of the petrochemistry and origin of the South Mountain Batholith and associated plutons, Nova Scotia, Canada. *In: High Heat Production (HHP) Granites, Hydrothermal Circulation and Ore Genesis. Institute of Mining and Metallurgy, England: 41-54.*
- Clarke, D.B., MacDonald, M.A., and Tate, M.C. 1997. Late Devonian mafic-felsic magmatism in the Meguma Zone, Nova Scotia. *In: The Nature of Magmatism in the Appalachian Orogen. Edited by A.K. Sinha, J.B. Whalen, and J.P. Hogan. Geological Society of America, Memoir 191: 107-127.*
- Dallmeyer, R.D. and Keppie, J.D. 1987. Polyphase late Paleozoic tectonothermal evolution of the southwestern Meguma Terrane, Nova Scotia: evidence from $^{40}\text{Ar}/^{39}\text{Ar}$ mineral ages. *Canadian Journal of Earth Sciences*, **24**: 1242-1254.
- Gray, P.D. 1996. Deformation and Metamorphism in the Contact Aureole of the South Mountain Batholith, Bedford area. B.Sc. thesis, Dalhousie University, 64p.
- Hicks, R. J., Jamieson, R.A., and Reynolds, P.H. (submitted). Detrital and metamorphic $^{40}\text{Ar}/^{39}\text{Ar}$ ages from muscovite and whole-rock samples, Meguma Supergroup, southern Nova Scotia. *Canadian Journal of Earth Sciences*.

- Horne, R.J., MacDonald, M.A., Corey, M.C., and Ham, L.J. 1992. Structure and emplacement of the South Mountain Batholith, southwestern Nova Scotia. *Atlantic Geology*, **28**: 29-50.
- Hutcheon, I. 1979. Sulphide-oxide-silicate Equilibria; Snow Lake, Manitoba. *American Journal of Science*, **279**: 643-665.
- Jamieson, R.A. 1974. The contact of the South Mountain Batholith near Mount Uniacke, Nova Scotia. B.Sc. thesis, Dalhousie University, 52p.
- Jones, R.A. 1997. Relative rates of sulphide oxidation by chemical and microbial means: The role of mineralogy and texture in acid rock drainage (ARD) from the Meguma Supergroup, Nova Scotia. B.Sc. thesis, Dalhousie University, 103p.
- Keppie, J.D. 1982. The Minas Geofracture. *In: Major Structural Zones and Faults of the Northern Appalachians. Edited by P. St. Julien and J. Béland. Geological Association of Canada, Special Paper 24*, pp. 263-280.
- MacDonald, M.A., Horne, J.R., Corey, M.C., and Ham, L.J. 1992. An overview of recent bedrock mapping and follow-up petrological studies of the South Mountain Batholith, southwestern Nova Scotia, Canada. *Atlantic Geology*, **28**: 7-29.
- Mahoney, K.L. 1996. The contact metamorphic aureole of the South Mountain Batholith, Nova Scotia. M.Sc. thesis, Acadia University, 118p.
- McKenzie, C.B. and Clarke, D.B. 1975. Petrology of the South Mountain Batholith, Nova Scotia. *Canadian Journal of Earth Sciences*, **12**: 1209-1218.
- Mohr, D.W., and Newton, R.C. 1983. Kyanite-Staurolite metamorphism in sulphidic schists of the Anakeesta Formation, Great Smoky Mountains, North Carolina. *American Journal of Science*, **283**: 97-134.

- Nance, R.D. 1987. Dextral transpression and late Carboniferous sedimentation in the Fundy Coastal Zone of southern New Brunswick. *In: Sedimentary basins and basin-forming mechanisms. Edited by C. Beaumont and A.J. Tankard. Canadian Society of Petroleum Geologists, Memoir 12: 363-377.*
- Pattison, D.R.M. and Tracy, R.J. 1991. Phase Equilibria and Thermobarometry of Metapelites. *In: Chapter 4 of Contact Metamorphism. Edited by D.M. Kerrick. Mineralogical Society of America, Reviews in Mineralogy, 26: 105-206.*
- Richardson, J.M., Bell, K., Blenkinsop, J., and Watkinson, D.H. 1989. Rb-Sr age and geochemical distinctions between the Carboniferous tin-bearing Davis Lake Complex and the Devonian South Mountain Batholith, Meguma Terrane, Nova Scotia. *Canadian Journal of Earth Sciences, 26:2044-2061.*
- Robinson, C. 1996. Pyrrhotite composition and its relationship to acid drainage potential in the Halifax Formation, Meguma Group, Nova Scotia. B.Sc. thesis, Dalhousie University, 72p.
- Schenk, P.E. 1983. The Meguma Terrane of Nova Scotia, Canada - An aid trans-Atlantic correlations *In: Regional Trends in the Geology of the Appalachian-Caledonian-Hercynian-Mauritanide Orogen. Edited by P.E. Schenk. D. Reidel Publishing Company, pp. 121-130.*
- Schenk, P.E. 1991. Events and sea-level changes on Gondwana's margin: The Meguma Zone (Cambrian to Devonian) of Nova Scotia, Canada. *Geological Society of America Bulletin, 103: 512-521.*
- Schenk, P.E. 1995a. Annapolis Belt *In: Chapter 4 of Geology of the Appalachian-Caledonian Orogen in Canada and Greenland. Edited by H. Williams. Geological Survey of Canada, Geology of Canada, 6: 367-383. (also Geological Society of America, The Geology of North America, v. F-1).*
- Schenk, P.E. 1995b. Meguma Zone *In: Chapter 3 of Geology of the Appalachian-Caledonian Orogen in Canada and Greenland. Edited by H. Williams. Geological Survey of Canada, Geology of Canada, 6: 261-277. (also Geological Society of America, The Geology of North America, v. F-1).*

- Smith, T.E. 1979. The geochemistry and origin of the Devonian granitic rocks of southwest Nova Scotia. *Geological Society of America Bulletin*, **90**: 850-885.
- Smith, T.E., and Turek, A. 1976. Tin-bearing potential of some Devonian granitic rocks in southwest Nova Scotia. *Mineralium Deposita*, **11**: 234-245.
- Tracy, R.J. and Robinson, P. 1988. Silicate-Sulphide-Oxide-fluid reactions in granulite-grade pelitic rocks, Central Massachusetts. *American Journal of Science*, **288A**: 45-74.
- Waldron, J.W.F. 1987. Sedimentology of the Goldenville-Halifax transition in the Tancook Island area, South Shore, Nova Scotia. *Geological Survey of Canada Open-file 1535*: 49
- Yardley, B. W. D. 1989. *An Introduction to Metamorphic Petrology*. Longman Group Limited, England.

Sample Descriptions

SAMPLE #	BB-97-2
LOCATION	Fairmont
ORIENTATION ANGLE	NA
PORPHYROBLASTS	and & cord
MODAL PERCENTAGES	30% (and.) 20% (cord.)
MATRIX COMPOSITION	qtz, musc., biot., opaques
OTHER	biot. concentrated around cord.

SAMPLE #	BB-97-3
LOCATION	Fairmont
ORIENTATION ANGLE	NA
PORPHYROBLASTS	sulphides
MODAL PERCENTAGES	15%
MATRIX COMPOSITION	qtz, musc., biot.
OTHER	preferred orientation of musc. and sulphides, inclusions in sulphides

SAMPLE #	BB-97-4
LOCATION	Fairmont
ORIENTATION ANGLE	160 ⁰
PORPHYROBLASTS	and. & cord.
MODAL PERCENTAGES	20% (and.) 10% (cord.)
MATRIX COMPOSITION	qtz, opaques, sericite, musc.
OTHER	inclusions in cord., some hexagonal cord. crystals

SAMPLE #	BB-97-5a & BB-97-5b
LOCATION	Northwest Arm Drive
ORIENTATION ANGLE	NA
PORPHYROBLASTS	and., cord., sulphides
MODAL PERCENTAGES	5% (and.) 15% (cord.) 5% (sulphides)
MATRIX COMPOSITION	qtz, biot., sericite, musc.
OTHER	biot. Rimming cord., very altered

SAMPLE #	BB-97-6
LOCATION	Main Street
ORIENTATION ANGLE	NA
PORPHYROBLASTS	and. & cord.
MODAL PERCENTAGES	30% (and.) 20% (cord.)
MATRIX COMPOSITION	qtz, musc., biot., sericite
OTHER	preferred orientation of cord. & musc.

SAMPLE #	BB-97-7
LOCATION	Dunbrack Street
ORIENTATION ANGLE	238 ⁰
PORPHYROBLASTS	cord. & sulphides
MODAL PERCENTAGES	20%(cord.) 10%(sulphides)
MATRIX COMPOSITION	qtz, biot., opaques
OTHER	foliation & opaques at 238 ⁰

SAMPLE #	BB-97-8
LOCATION	Exit 1A, Highway 102
ORIENTATION ANGLE	170 ⁰
PORPHYROBLASTS	and. & cord.
MODAL PERCENTAGES	20% (and.) 10% (cord.)
MATRIX COMPOSITION	qtz, biot., musc., opaques
OTHER	sulphides at 170 ⁰

SAMPLE #	BB-97-10
LOCATION	Exit 1A, Highway 102
ORIENTATION ANGLE	187 ⁰
PORPHYROBLASTS	and. & biot. & cord.
MODAL PERCENTAGES	30% (and.) 25% (biot.) 10% (cord.)
MATRIX COMPOSITION	qtz, musc., sericite, opaques
OTHER	opaques rim and., biot. Rims opaques

SAMPLE #	BB-97-11
LOCATION	Exit 1A, Highway 102
ORIENTATION ANGLE	NA
PORPHYROBLASTS	sulphides
MODAL PERCENTAGES	15%
MATRIX COMPOSITION	qtz, musc., biot.
OTHER	

SAMPLE #	BB-97-12
LOCATION	Exit 1A, Highway 102
ORIENTATION ANGLE	264 ⁰
PORPHYROBLASTS	and. & cord.
MODAL PERCENTAGES	25% (and.) 25% (cord.)
MATRIX COMPOSITION	qtz, biot., opaques, sericite
OTHER	elongate and. crystals at 174 ⁰ , opaques rim and

SAMPLE #	BB-97-13
LOCATION	Exit 1A, Highway 102
ORIENTATION ANGLE	086°
PORPHYROBLASTS	opaques & cord.
MODAL PERCENTAGES	20% (opaques) 10% (cord.)
MATRIX COMPOSITION	qtz, biot.
OTHER	fabric at 086°

SAMPLE #	BB-97-14
LOCATION	Lovette Lake Court
ORIENTATION ANGLE	NA
PORPHYROBLASTS	and.
MODAL PERCENTAGES	5%
MATRIX COMPOSITION	qtz (20%), opaques (10%), micas (60%)
OTHER	

SAMPLE #	BB-97-15
LOCATION	Lovette Lake Court
ORIENTATION ANGLE	303°
PORPHYROBLASTS	and.
MODAL PERCENTAGES	20%
MATRIX COMPOSITION	qtz, biot., chlor., musc.
OTHER	

SAMPLE #	BB-97-16
LOCATION	Lovette Lake Court
ORIENTATION ANGLE	NA
PORPHYROBLASTS	and.
MODAL PERCENTAGES	20%
MATRIX COMPOSITION	qtz, opaques, sericite
OTHER	

SAMPLE #	BB-97-17
LOCATION	Lovette Lake Court
ORIENTATION ANGLE	NA
PORPHYROBLASTS	NA
MODAL PERCENTAGES	NA
MATRIX COMPOSITION	qtz, biot., musc., chlor., and., sulphides
OTHER	coarse, subhedral qtz,

SAMPLE #	BB-97-18
LOCATION	Otter Lake Crescent
ORIENTATION ANGLE	140 ⁰
PORPHYROBLASTS	and.
MODAL PERCENTAGES	10%
MATRIX COMPOSITION	qtz, sericite, opaques
OTHER	

SAMPLE #	BB-97-19
LOCATION	Otter Lake Crescent
ORIENTATION ANGLE	108 ⁰
PORPHYROBLASTS	NA
MODAL PERCENTAGES	NA
MATRIX COMPOSITION	qtz, musc., biot., chlor
OTHER	schist - 80% mica

SAMPLE #	BB-97-20
LOCATION	Otter Lake Crescent
ORIENTATION ANGLE	078 ⁰
PORPHYROBLASTS	and.
MODAL PERCENTAGES	15%
MATRIX COMPOSITION	qtz, sulphides, biot., musc.
OTHER	few altered feldspars

SAMPLE #	BB-97-21
LOCATION	behind Kmart, Bayers Lake Industrial Park
ORIENTATION ANGLE	NA
PORPHYROBLASTS	NA
MODAL PERCENTAGES	NA
MATRIX COMPOSITION	qtz, biot., musc., opaques, sericite
OTHER	

SAMPLE #	BB-97-22
LOCATION	behind Kmart, Bayers Lake Industrial Park
ORIENTATION ANGLE	300 ⁰
PORPHYROBLASTS	NA
MODAL PERCENTAGES	NA
MATRIX COMPOSITION	fine-grained equant qtz
OTHER	sericite, chlor. veining

Abbreviations:

qtz (quartz)

and. (andalusite)

cord. (cordierite)

musc. (muscovite)

biot. (biotite)

chlor. (chlorite)

JOEL 733 Electron Microprobe

Department of Earth Sciences
Dalhousie University

Analytical Methods:

Analyses were carried out on a JOEL 733 electron microprobe equipped with four wavelength dispersive spectrometers and an Oxford Link eXL energy dispersive system. The energy dispersive system was used for all elements. Resolution of the energy dispersive detector was 137eV at 5.9KeV. Each spectrum was acquired for 40 seconds with an accelerating voltage of 15 Kv and a beam current of 15 nA. Probe spot size was approximately 1 micron. The raw data was corrected using Link's ZAF matrix correction program.

Instrument calibration was performed on cobalt metal.

Instrument precision on cobalt metal (n=10) was +/- .5% at 1 standard deviation.

Accuracy for major elements was +/- 1.5 to 2.0% relative. Geological standards were used as controls. Detection limits for most elements using the energy dispersive system range from approximately 0.1 to 0.3 percent.

Andalusite

Sample #	BB-97-2	BB-97-2	BB-97-2	BB-97-2	BB-97-2	BB-97-5b	BB-97-5b	BB-97-5b
Analysis #	1	2	3	4	5	1	2	3
Group #	3	3	3	3	3	NA	NA	NA
wt % oxide								
SiO ₂	37.1	37.22	37	36.78	37.18	36.13	35.95	36.96
Al ₂ O ₃	62.83	63.21	61.56	63.53	62.86	63.58	63.47	62.81
FeO			1.06					
total	99.93	100.43	99.62	100.31	100.04	99.71	99.42	99.77
Si	1	1	1.005	0.99	1	0.98	0.975	1
Al	2	2	1.975	2.015	1.995	2.03	2.03	2
Fe	0	0	0.025	0	0	0	0	0
total cations	3	3	3.005	3.005	2.995	3.01	3.005	3

Garnet

Sample #	BB-97-1.1	BB-97-1.1	BB-97-1.1
Analysis #	4	8	9
Group #	NA	NA	NA
wt% oxide			
SiO ₂	37.11	37.52	37.99
Al ₂ O ₃	20.7	20.4	20.99
FeO	27.17	26.2	28.55
MnO	12.02	11.61	9.94
MgO	1.65	1.96	2.64
CaO	1.13	1.49	1.29
total	99.78	99.18	101.4
Si	3.024	3.06	3.024
Al	1.992	1.956	1.968
Fe	1.848	1.788	1.896
Mn	0.828	0.804	0.672
Mg	0.204	0.24	0.312
Ca	0.096	0.132	0.108
total cations	7.992	7.98	7.98
A	0.418013	0.420099	0.402261
M	0.057252	0.069602	0.084643
Fe/Fe + Mg	0.942748	0.930398	0.915357

Biotite

Sample #	BB-97-1.1	BB-97-1.1	BB-97-1.2	BB-97-1.2	BB-97-2	BB-97-2	BB-97-2	BB-97-3
Analysis #	11	12	1	2	6	7	8	5
Group #	NA	NA	NA	NA	3	3	3	5
wt % oxide								
SiO2	34.16	35.25	35.81	35.34	36.22	35.86	35.93	35.19
TiO2	2.66	2.52	3.5	3.14	2.04	2.14	2.57	2.12
Al2O3	19.1	19.43	19.71	19.67	19.66	20.02	18.72	19.22
FeO	20.3	20.21	21.06	19.97	19.45	18.86	18.37	20.86
MnO	0.34	0.48	0.33	0.31	0	0	0	0
MgO	7.67	7.48	7.05	6.63	8.82	9.22	8.62	7.94
Na2O	0.26	0	0	0.41	0	0	0	0
K2O	8.49	9.35	7.85	9.02	7.85	8.55	8.46	8.3
total	92.98	94.72	95.31	94.49	94.04	94.65	92.67	93.63
Si	5.346	5.412	5.434	5.434	5.5	5.434	5.544	5.456
Ti	0.308	0.286	0.396	0.374	0.242	0.242	0.308	0.242
Al	3.52	3.52	3.52	3.564	3.52	3.564	3.388	3.498
Fe	2.662	2.596	2.662	2.574	2.464	2.398	2.376	2.706
Mn	0.044	0.066	0.044	0.044	0	0	0	0
Mg	1.782	1.716	1.584	1.518	2.002	2.09	1.98	1.826
Na	0.088	0	0	0.132	0	0	0	0
K	1.694	1.826	1.518	1.76	1.518	1.65	1.672	1.65
total cations	15.444	15.422	15.158	15.4	15.246	15.378	15.268	15.378
A	-0.29491	-0.45202	-0.15822	-0.3847	-0.15956	-0.25078	-0.32759	-0.24567
M	0.274222	0.270134	0.2508	0.249248	0.311992	0.328348	0.319378	0.275694
Fe/Fe + Mg	0.725778	0.729866	0.7492	0.750752	0.688008	0.671652	0.680622	0.724306

BB-97-5b	BB-97-5b	BB-97-5b	BB-97-7.1	BB-97-7.1	BB-97-7.1	BB-97-7.1	BB-97-7.2	BB-97-7.2
5	7	9	5	6	7	8	2	4
NA	NA	NA	5	5	5	5	5	5
35.91	34.2	35.76	34.86	36.07	35.7	36.14	36.07	35.99
3.05	2.3	2.66	2	1.67	2.01	1.56	2.02	1.7
19.28	18.72	19.11	20.14	19.64	20.48	19.57	19.2	19.77
20.25	19.49	19.82	17	16.48	15.22	16.45	17.04	16.49
0	0	0	0	0	0.41	0.3	0	0.31
7.72	7.93	8.04	11.72	11.14	9.24	11.67	11.39	11.58
0.25	0.29	0	0	0	0.251	0.27	0.34	0
9.11	8.61	8.79	6.98	7.71	7.54	7.71	7.79	7.94
95.57	91.54	94.18	92.7	92.71	90.851	93.67	93.85	93.78
5.456	5.412	5.478	5.302	5.478	5.5	5.456	5.456	5.434
0.352	0.264	0.308	0.22	0.198	0.242	0.176	0.22	0.198
3.454	3.498	3.454	3.608	3.52	3.718	3.476	3.41	3.52
2.574	2.574	2.552	2.156	2.09	1.958	2.068	2.156	2.09
0	0	0	0	0	0.044	0.044	0	0.044
1.738	1.87	1.848	2.662	2.53	2.134	2.618	2.574	2.596
0.066	0.088	0	0	0	0.066	0.088	0.11	0
1.76	1.738	1.716	1.364	1.496	1.474	1.474	1.496	1.518
15.4	15.444	15.356	15.312	15.312	15.136	15.4	15.422	15.4
-0.4041165	-0.35007	-0.35243	-0.02865	-0.14463	-0.09588	-0.14495	-0.17189	-0.16861
0.27601001	0.289205	0.288586	0.408078	0.403331	0.37776	0.415007	0.400633	0.41254
0.72398999	0.710795	0.711414	0.591922	0.596669	0.62224	0.584993	0.599367	0.58746

Cordierite

Sample #	BB-97-1.1	BB-97-1.1	BB-97-1.2	BB-97-2	BB-97-2	BB-97-2	BB-97-5b	BB-97-5b
Analysis #	5	13	4	1	2	4	11	12
Group #	NA	NA	NA	3	3	3	NA	NA
wt % oxide								
SiO ₂	40.24	42.72	48.21	47.76	48.89	49.06	48.56	49.16
Al ₂ O ₃	26.71	30.32	32.27	32.16	32.64	33.2	32.54	32.65
FeO	11.3	5.84	9.19	8.91	9.51	9.49	9.54	9.91
MnO	0.3	0	1.36	0.33		0.27	0.43	
MgO	6.79	3.26	6.38	7.18	7.16	7.62	7.22	6.9
CaO	0.68	0	0	0	0	0	0	0
K ₂ O	1.26	6.37	0	0	0	0	0	0
Na ₂ O		0.214	0.55	0.31		0.3	0.31	0.33
total	87.28	88.724	97.96	96.65	98.2	99.94	98.6	98.95
Si	4.86	5.022	5.04	5.022	5.058	5.004	5.022	5.058
Al	3.798	4.194	3.978	3.996	3.978	3.996	3.96	3.96
Fe	1.134	0.576	0.81	0.792	0.828	0.81	0.828	0.846
Mn	0.036	0	0.126	0.036	0	0.018	0.036	0
Mg	1.224	0.576	0.99	1.134	1.098	1.152	1.116	1.062
Ca	0.09	0	0	0	0	0	0	0
K	0.198	0.954	0	0	0	0	0	0
Na	0	0.054	0.108	0.072	0	0.054	0.072	0.072
total cations	11.34	11.376	11.052	11.052	10.962	11.034	11.034	10.998
A	0.558996	0.551945	0.67454	0.666528	0.661935	0.659909	0.660041	0.660129
M	0.375345	0.358242	0.409762	0.44624	0.429514	0.445354	0.430788	0.41047
Fe/Fe +Mg	0.624655	0.641758	0.590238	0.55376	0.570486	0.554646	0.569212	0.58953

Sample #	BB-97-5b	BB-97-7.1	BB-97-7.1	BB-97-7.1	BB-97-7.1
Analysis #	13	1	2	3	4
Group #	NA	5	5	5	5
wt % oxide					
SiO ₂	48.52	48.52	50.43	48.49	48.59
Al ₂ O ₃	32.75	32.8	32.12	32.84	33.04
FeO	9.82	6.92	6.94	7.18	7.1
MnO	0.44	0.7	0.72	0.75	0.62
MgO	7.1	8.64	8.38	8.74	8.57
CaO	0	0	0	0	0
K ₂ O		0	0	0	0
Na ₂ O	0.45	0.47	0.29	0.33	0.52
total	99.08	98.05	98.88	98.33	98.44
Si	5.004	5.004	5.13	4.986	4.986
Al	3.978	3.978	3.852	3.978	3.996
Fe	0.846	0.594	0.594	0.612	0.612
Mn	0.036	0.054	0.054	0.072	0.054
Mg	1.098	1.332	1.278	1.332	1.314
Ca	0	0	0	0	0
K	0	0	0	0	0
Na	0.09	0.09	0.054	0.072	0.108
total cations	11.052	11.052	10.962	11.052	11.07
A	0.659352	0.678246	0.677066	0.673503	0.6783
M	0.419622	0.55527	0.546997	0.548995	0.546905
Fe/Fe +Mg	0.580378	0.44473	0.453003	0.451005	0.453095

Plagioclase

Sample #	BB-97-1.1	BB-97-1.1	BB-97-3	BB-97-7.1	BB-97-7.2
Analysis #	5	6	9	3	5
Group #	NA	NA	5	5	5
wt% oxide					
Si O2	62.95	63.26	66.61	65.19	64.82
Al2O3	24.26	24.54	21.28	22.28	22.05
CaO	5.42	5.5	1.59	3.17	3.17
Na2O	8.3	7.31	9.45	8.6	9.75
Feo	0	0	0.3	0	0
P2O5	0	0	0.43	0	0
Total	100.93	100.61	99.66	99.24	99.79
Si	2.76	2.768	2.912	2.872	2.856
Al	1.256	1.264	1.096	1.16	1.144
Ca	0.256	0.256	0.072	0.152	0.152
Na	0.704	0.624	0.8	0.736	0.832
Fe	0	0	0.008	0	0
P	0	0	0.016	0	0
total cations	4.976	4.912	4.904	4.92	4.984

K-Feldspar

Sample #	BB-97-2	BB-97-2
Analysis #	9	3
Group #	3	3
wt % oxide		
SiO2	64.52	63.99
Al2O3	18.94	18.27
Na2O	1.38	1.45
K2O	13.63	12.73
P2O5	0.85	0
total	99.32	96.44
Si	2.96	3.016
Al	1.024	1.016
Na	0.12	0.136
K	0.8	0.768
P	0.032	0
total cations	4.936	4.936

Muscovite

Sample #	BB-97-1.1	BB-97-2	BB-97-5b	BB-97-5b	BB-97-7.2
Analysis #	14	10	14	15	1
Group #	NA	3	NA	NA	5
wt % oxide					
SiO ₂	47.75	47.06	47.27	48.16	47.13
TiO ₂	0	0.68	0.64	0.5	0.27
Al ₂ O ₃	30.83	36.08	35.76	37.09	36.93
FeO	5.27	0.9	1.08	1.03	0.55
MgO	2.69	0.47	0.72	0.48	0.53
Na ₂ O	0	0.32	0.36	0.45	0.65
K ₂ O	8.06	7.93	7.63	7.84	7.35
total	94.6	93.44	93.46	95.55	93.41
Si	6.424	6.248	6.27	6.248	6.226
Ti	0	0.066	0.066	0.044	0.022
Al	4.884	5.654	5.588	5.676	5.742
Fe	0.594	0.11	0.11	0.11	0.066
Mg	0.55	0.088	0.132	0.088	0.11
Na	0	0.088	0.088	0.11	0.176
K	1.386	1.342	1.298	1.298	1.232
total cations	13.838	13.596	13.552	13.574	13.574

Chalcopyrite

Sample #	BB-97-3	BB-97-5b
Analysis #	6	3
Group #	5	NA
Atom. %		
Cu	24.64	24.52
Fe	25.55	25.75
S	49.7	49.72
total	99.89	99.99
Formula	Cu _{0.99} Fe _{1.03} S ₂	Cu _{0.99} Fe _{1.03} S ₈

Ilmenite

Sample #	BB-97-1	BB-97-2	BB-97-7.1
Analysis #	3	2	4
Group #	NA	3	5
Atom. %			
Fe	39.66	47.95	38.07
Mn	10.23	1.97	10.46
Ti	50.09	50.08	48.83
total	99.98	100	97.36
Formula	(Fe _{0.8} Mn _{0.2})TiO ₃	(Fe _{0.96} Mn _{0.04})TiO ₃	(Fe _{0.78} Mn _{0.21})TiO ₃

Pyrite

Sample #	BB-97-3	BB-97-3	BB-97-3	BB-97-3	BB-97-7.1
Analysis #	1	2	3 3b		1
Group #	5	5	5	5	5
Atom. %					
Fe	34.09	33.61	35.52	33.63	33.5
S	65.66	66.33	64.35	66.3	66.37
total	99.75	99.94	99.87	99.93	99.87
Formula	Fe _{1.04} S ₂	Fe _{1.01} S ₂	Fe _{1.1} S ₂	Fe _{1.01} S ₂	Fe _{1.01} S ₂

Sample #	BB-97-7.1	BB-97-7.1
Analysis #	2	3
Group #	5	5
Atom. %		
Fe	32.46	33.16
S	67.37	66.74
total	99.83	99.9
Formula	Fe _{0.96} S ₂	Fe _{0.99} S ₂

Pyrrhotite

Sample #	BB-97-1	BB-97-1	BB-97-1	BB-97-2	BB-97-2	BB-97-3	BB-97-3
Analysis #	1	2	4	1	3	4	5
Group #	NA	NA	NA	3	3	5	5
Atom. %							
Fe	46.88	46.65	47.21	46.75	46.3	46.96	47.06
S	53.05	52.84	52.79	53.18	53.48	52.75	52.67
total	99.93	99.49	100	99.93	99.78	99.71	99.73
Formula	Fe7.07S8	Fe7.06S8	Fe8.9S10	Fe7.03S8	Fe6.9S8	Fe8.9S10	Fe8.9S10
Sample #	BB-97-3	BB-97-5b	BB-97-5b	BB-97-5b	BB-97-7.2	BB-97-7.2	BB-97-7.2
Analysis #	2	1	2	4	1	2	3
Group #	5	NA	NA	NA	5	5	5
Atom. %							
Fe	46.91	47.4	47.54	47.36	46.21	46.46	46.34
S	52.99	52.52	52.39	52.54	53.58	53.47	53.57
total	99.9	99.92	99.93	99.9	99.79	99.93	99.91
Formula	Fe7.08S8	Fe9S10	Fe9.1S10	Fe9S10	Fe6.9S8	Fe6.95S8	Fe6.92S8